ELSEVIER

Tectonophysics 308 (1999) 143–170

TECTONOPHYSICS

www.elsevier.com/locate/tecto

The Holocene paleoearthquakes on the 1915 Avezzano earthquake faults (central Italy): implications for active tectonics in the central Apennines

F. Galadini [a,*], P. Galli [b]

[a] CNR, Istituto di Ricerca sulla Tettonica Recente, Area di Ricerca di Roma-Tor Vergata, via del Fosso del Cavaliere, 00133 Rome, Italy
[b] Servizio Sismico Nazionale, via Curtatone 3, 00185 Rome, Italy

Received 4 October 1998; accepted 27 November 1998

Abstract

Extensive paleoseismological research was conducted in the Fucino Plain (central Italy) in order to better understand the seismogenic characteristics of the fault responsible for the 1915 Avezzano earthquake ($M_s = 7.0$) and improve the general knowledge regarding active tectonics in the central Apennines. Evidence for Late Pleistocene–Holocene surface faulting events was obtained through the study of thirteen sites across four different fault branches. The paleoseismological analysis outlined the occurrence of ten surface faulting events in the past 33,000 years, seven of which occurred during the Holocene. Radiocarbon, thermoluminescence and archaeological dating permitted the definition of an event chronology and the estimation of a recurrence interval for surface faulting events ranging between 1400 and 2600 years. On the basis of the observed offsets it was possible to calculate vertical slip rates for the individual fault branches, ranging between 0.24 mm yr^{-1} and 0.5 mm yr^{-1} and an extension rate across the Fucino Plain ranging between 0.6 and 1 mm yr^{-1}. The chronology of surface faulting events appears linearly distributed in time, and the observed recurrence times are similar to those inferred by other paleoseismological studies along different active Apennine faults. The general consequence of the large time span between strong earthquakes is that even a 2000 year long historical record, such as the Italian earthquake catalogue, does not cover the entire seismic cycle of all the active Apennine faults. A comparison of the extension rate across the Fucino Plain with that across the entire central Apennines (as inferred from the sum of seismic moments of earthquakes which occurred in the interval 1000–1992) shows a seismicity 'deficit' in the period indicated. This confirms that a number of seismogenic faults were not active during the past 1000 years.

Keywords: active fault; paleoseismology; earthquakes; seismotectonics; Apennines

1. Introduction

The 1915 Avezzano earthquake ($M_s = 7.0$, according to Margottini et al., 1993), which struck the Fucino Plain (central Italy), is one of the major seismic events to have occurred in Italy over the last few centuries. Due to its relatively recent occurrence, the coseismic effects are well known in terms of intensity distribution (for example it was responsible for damage in Rome) and descriptions and a map of surface ruptures are included in the fundamental work of Oddone (1915).

Although the occurrence of strong earthquakes

* Corresponding author. Fax: +39-6-4993-4211; E-mail: galad@irtr.rm.cnr.it

0040-1951/99/$ – see front matter
PII: S0040-1951(99)00091-8

along the Apennine chain is described in the Italian seismic catalogues (e.g. Boschi et al., 1997; Camassi and Stucchi, 1997), the seismogenic behaviour of the faults responsible for these earthquakes is not well known. For the 1915 earthquake area, reliable data on the recurrence intervals between large seismic events and slip or extension rates across the Fucino basin are lacking. According to seismic catalogues the 1915 event occurred in an area where apparently no other earthquakes had originated during the last millennium. This observation is not surprising if one considers that paleoseismological data from central-southern Italy (e.g. Pantosti et al., 1996) show that coseismic faulting within the Apennine chain may be characterised by long recurrence intervals (1000 years or more along the same active fault). The lack of other large historical earthquakes in the Fucino Plain may therefore be due to the long recurrence intervals for 1915-type events.

Extensive paleoseismological research has been performed during 1992–1996 to better understand the seismogenic behaviour of the structure responsible for the 1915 earthquake. The paleoseismological analysis was based on diverse investigations: (1) the study of twelve trenches excavated ad hoc along the major Holocene fault branches; (2) the study of the displacements of Holocene sediments in two quarries located at the eastern edge of the plain; (3) the survey of excavations dug for the laying of a pipeline and an aqueduct (in the northeastern and southwestern sectors of the basin, respectively); (4) the survey of some drainage channels in the central part of the basin; (5) the examination of hundreds of shallow boreholes (3–4 m deep); and (6) the analysis of coseismic deformations affecting archaeological remains. Collected data have already been published in several papers (Galadini et al., 1995, 1996, 1997; Galadini and Galli, 1996).

The paleoseismological investigation was preceded by the reconstruction of the Quaternary geological and tectonic evolution of the region through detailed stratigraphic, geomorphological and structural work (Galadini and Messina, 1994). Particular attention was also given to the geological evolution of the Late Pleistocene and Holocene through the study of the lacustrine terraces and related deposits which surround the Fucino Plain (Giraudi, 1988).

Based on the large amount of available data, the present paper addresses active-faulting problems in an effort to understand the characteristics of the present tectonic regime and to provide insight for seismic hazard assessment in the central Apennines. All data on the active tectonics of the Fucino Plain collected during the last 10 years have been synthesised in the present paper. The results of the paleoseismological analysis are presented in the article in different sections, with each section relating to a major Holocene fault branch within the Fucino Plain. The implications derived from the paleoseismological analysis (e.g. slip rates, recurrence intervals for large seismic events, inferred 1915 surface-faulting, etc.) are discussed in specific sections.

2. Geological framework

The structure of the central Apennines is mainly due to Cenozoic compressive tectonics which produced intense shortening across NW–SE trending thrust faults (e.g. CNR-PFG, 1983), the most important of which placed Meso–Cenozoic carbonates in contact with Miocene flysch. Since the Pliocene, the extensional regime related to the numerous 10–20 km-long, NW–SE trending normal faults has been responsible for the formation of the main intermontane basins (Fig. 1). These faults affect Quaternary continental deposits (mainly lacustrine and fluvial facies) and show spectacular carbonate bedrock fault scarps. Outside the intermontane basins Quaternary fault activity is observed in the displacement of slope-derived breccias or scree deposits. Slip rates calculated on the basis of the displacement of Early Pleistocene formations (along the VF, SVFZ and PF of Fig. 1) are less than 1 mm yr^{-1} (e.g. Galadini and Messina, 1994).

Bosi (1975) used a mainly geomorphological approach to define the faults reported in Fig. 1 as being ‘probably active’. Recent works (e.g. Galadini and Messina, 1994 and references therein; Carrara et al., 1995; Chiarini et al., 1997), however, provide better constraints on their activity (Fig. 1). Active faults are present throughout this sector of the Apennine chain and are characterised by the clear displacement of Late Pleistocene–Holocene deposits. In contrast, some faults which show geomorphic evidence of recent activity are sealed by middle Pleistocene de-

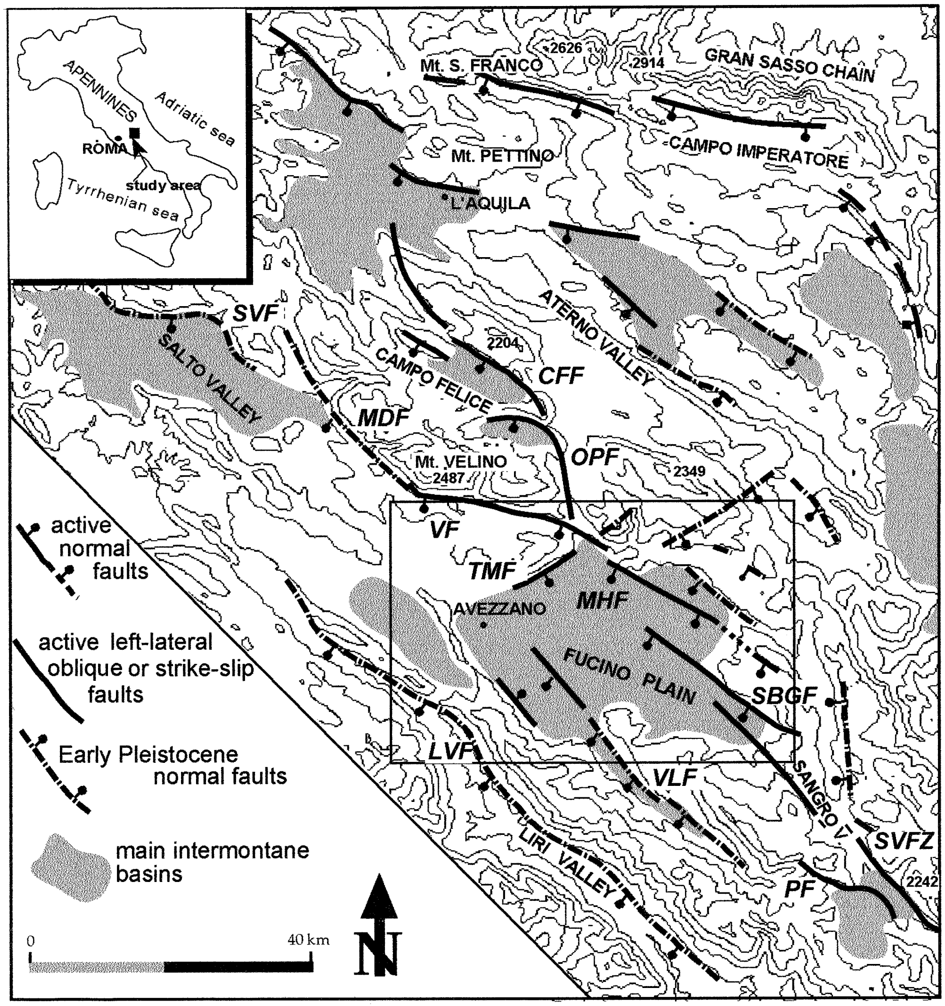

Fig. 1. Fault map of the Fucino Plain and surrounding areas. The rectangle encloses the study area of Fig. 2. *PF* = Pescasseroli fault; *SVFZ* = Sangro Valley fault zone; *VLF* = Vallelonga fault; *LVF* = Liri Valley fault; *SBGF* = San Benedetto dei Marsi–Gioia dei Marsi fault; *MHF* = Marsicana Hwy fault; *TMF* = Tre Monti fault; *VF* = Velino fault; *OPF* = Ovindoli-Pezza fault; *CFF* = Campo Felice fault; *MDF* = Monti della Duchessa fault; *SVF* = Salto Valley fault.

posits and landforms, and as such they are no longer considered to be active (e.g. the Liri Valley fault and the Monti della Duchessa fault; LVF and MDF, respectively, in Fig. 1).

The Fucino Plain (Fig. 2), one of the major intermontane basins of the central Apennines, is filled by more than 1000 m of lacustrine and fluvial Plio–Quaternary deposits and surrounded by mountains (average 2000 m) made of Meso–Cenozoic carbonate formations. Several terraces, which range in age from Pliocene to Holocene, are found at different elevations around the basin. Some of them represent the top surfaces of lacustrine sedimentary units while others are carved into older deposits.

According to Galadini and Messina (1994) the tectonic evolution of the Fucino basin started during the Pliocene, when NE–SW faults (TMF and its northeastern prolongation in Fig. 1) along the northern border formed a half-graben basin. Since the Late Pliocene, however, activity started on NW–SE trending fault branches located along the eastern border of the basin (Marsicana Hwy fault and San Benedetto dei Marsi–Gioia dei Marsi fault, MHF and SBGF, respectively, in Figs. 1 and 2) form-

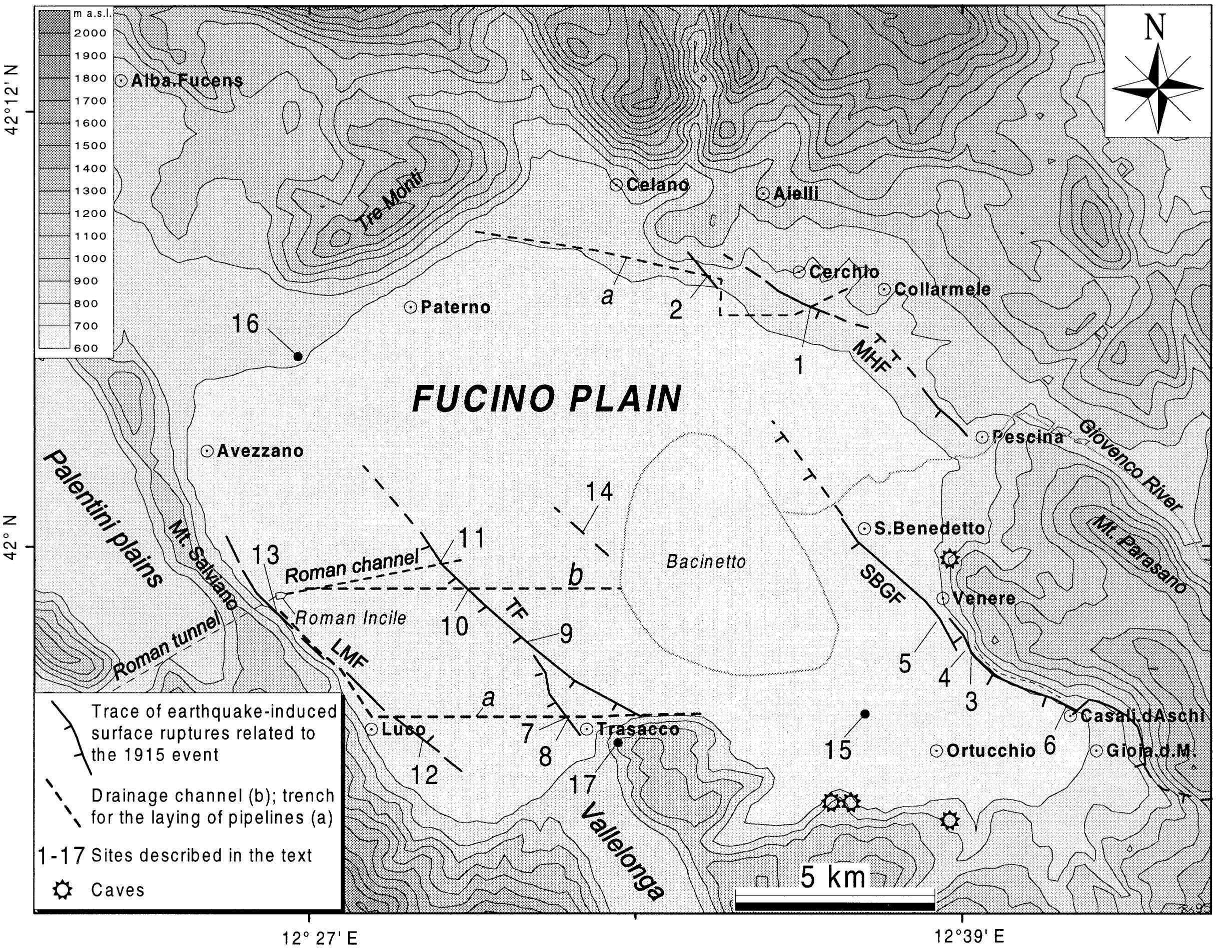

Fig. 2. Study area map showing site locations and the surface faulting pattern of the 1915 earthquake inferred from historical reports and the present paleoseismological study.

ing a new half-graben which was superimposed on and perpendicular to the pre-existing one. Data from reflection seismic surveys (e.g. Mostardini and Merlini, 1986) show the present half-graben structure with fill sediments which clearly pinch out along the western border of the basin and the listric geometry (typical of growth-faults) of the MHF and SBGF. The basin is also affected by secondary faults, the most important of which are the Trasacco and the Luco dei Marsi faults (TF and LMF, respectively, in Fig. 2).

The attempts to drain Lake Fucino have been a *leitmotif* of the last two millennia, beginning with the partial drainage of the lake by the ancient Romans (1st–2nd century A.D.). They constructed an impressive hydraulic system, consisting of a tunnel excavated in Mt. Salviano and open channels in the plain (Fig. 2), which ceased to operate during the decadence of the Empire (5th–6th century A.D.). Recent detailed stratigraphic and geomorphological investigations allowed Giraudi (1998) to reconstruct lake level oscillations for the last 30,000 years. Data related to the last two millennia show that the level has increased significantly only since the 14th century, culminating in peak levels during the 19th century when the lake was finally drained for agricultural purposes (1862–1875). Presently, the Fucino area is an essentially flat, intensely cultivated plain (Fig. 3) which is cut by many E–W and N–S trending drainage channels.

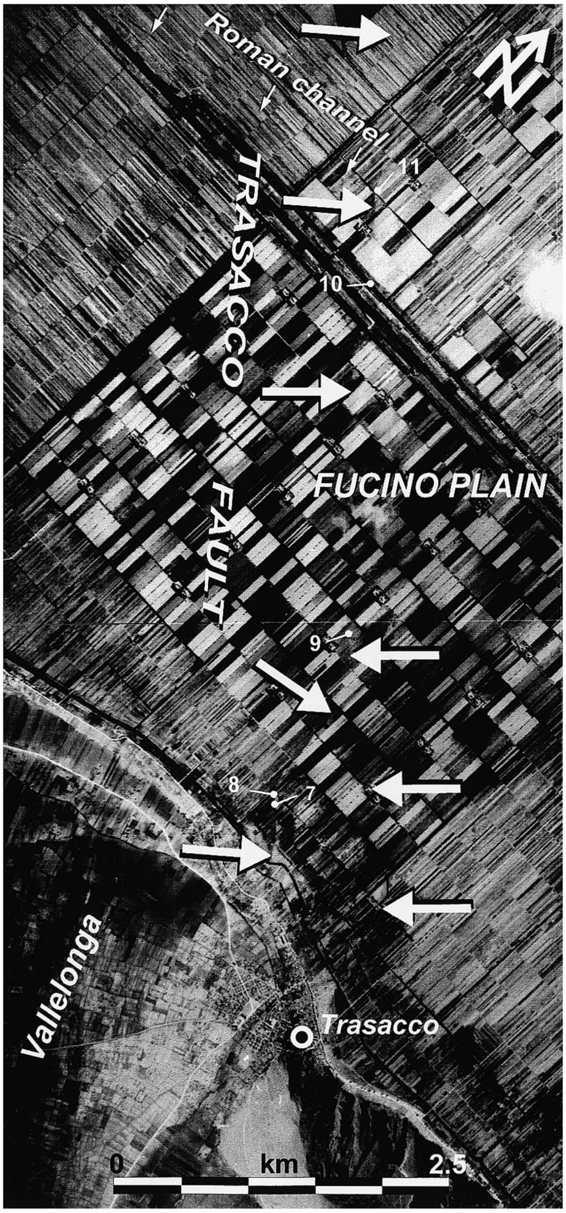

Fig. 3. Aerial photograph of the SE portion of the Fucino basin. Large arrows highlight the Trasacco fault (TF in the text), visible on the photograph as a faint lineament affecting the plain. The location of the study sites is reported along the fault. Small arrows indicate the trace of the Roman channel built in the 1st–2nd century A.D. to partially drain the lake.

The survey of the aqueduct trench in the south-western portion of the basin (Fig. 2) and of the walls of the present drainage channels (the main of which is reported in Fig. 2) and about 400, 4-m-deep hand-boreholes have been used to reconstruct the stratigraphic succession of the inner and western portions of the basin over the last 30,000 years. Four main sedimentary units have been distinguished, separated by erosional surfaces and dated by means of radiocarbon or archaeological analysis (Fig. 4). In contrast, a complete Late Pleistocene–Holocene stratigraphic record is not available for the eastern border of the basin, which is affected by the SBGF and MHF. This is due to lateral facies variability, as well as the abundance of erosional episodes and colluvial deposition along the Lake Fucino paleoshoreline.

Due to the evidence of recent tectonic activity along the above-mentioned faults, and the presence of very recent lacustrine sediments (up to the 19th century A.D.) which allow the characterization of displacement events, the Fucino Plain appears to be an ideal place for paleoseismological analysis.

3. The 1915 earthquake

On January 13, 1915 a strong earthquake ($M_s = 7.0$) struck the villages in the Fucino basin and surrounding areas, causing more than 30,000 casualties and strong damage over an area of 500 km^2. According to the Italian seismic catalogues (Boschi et al., 1997; Camassi and Stucchi, 1997) the main shock epicentre was located between Gioia dei Marsi and Ortucchio and the hypocentre occurred at a depth of 8 km. The earthquake was also responsible for the damage of some monuments in Rome, affecting 22 old churches, 20 old *palazzi*, several parts of the Aurelian walls and parts of the Claudius aqueduct.

The earthquake was recorded in several seismic stations world-wide; three proposed focal mechanisms based on first arrivals have been published for this earthquake, each showing totally different solutions: NE–SW normal faulting (Micci et al., 1975); NE–SW left-lateral strike-slip faulting (Gasparini et al., 1985); NW–SE left-lateral strike-slip faulting (Basili and Valensise, 1991). None of these solutions is sufficiently constrained because of the low quality of the original seismic records (for a detailed discussion, see Basili and Valensise, 1991). Moreover, all the proposed solutions clearly contrast the known

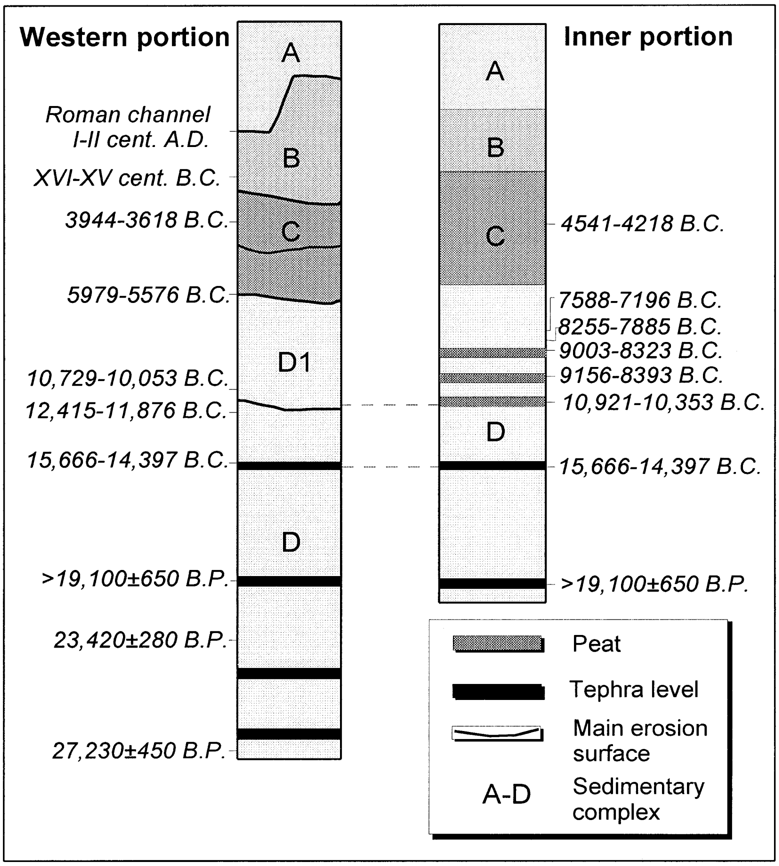

Fig. 4. Stratigraphic columns and related ages of lacustrine sediments (mainly silts and clays) in the western and inner portions of the plain.

structural framework of the Fucino area, which is characterised by NW–SE active normal faults.

A few days after the earthquake, Oddone (1915) provided a detailed field-based report of the surface ruptures (Fig. 5), he described the main scarp along the eastern border of the basin, with a maximum height of 1 m and lack of horizontal component of movement. According to Oddone, as well as to Alfani (1915) and other historical sources (including press reports), the main fault scarp affected the Marsicana Hwy between Cerchio and Pescina at two different locations. To the south, the main NW–SE scarp roughly followed the border of the historical lake (up to the Gioia dei Marsi area). Although Oddone's map clearly shows the presence of scarps also in the inner portion of the basin, no precise description of these features is reported in the text. As a matter of fact, Oddone's map (Fig. 5) highlights an almost continuous rupture with the downthrown side always located towards the centre of the plain. Other geologic effects affected the most damaged areas, including landslides in the southeastern part (close to Gioia dei Marsi), differential settlements in the inner portion and liquefactions along the eastern border of the basin (Galli and Ferreli, 1995).

More recently, Oddone's data were interpreted by Serva et al. (1986) using eye-witness accounts of the earthquake and new field surveys. The authors concluded that the two easternmost fault branches slipped in 1915: the Marsicana Hwy fault (MHF) and the San Benedetto dei Marsi–Gioia dei Marsi fault (SBGF) (Figs. 1 and 2). Using new historical and geologic data Galadini et al. (1995) confirmed this conclusion but pointed out that the surface faulting pattern of the 1915 earthquake — as reconstructed — could be still incomplete due to the lack of

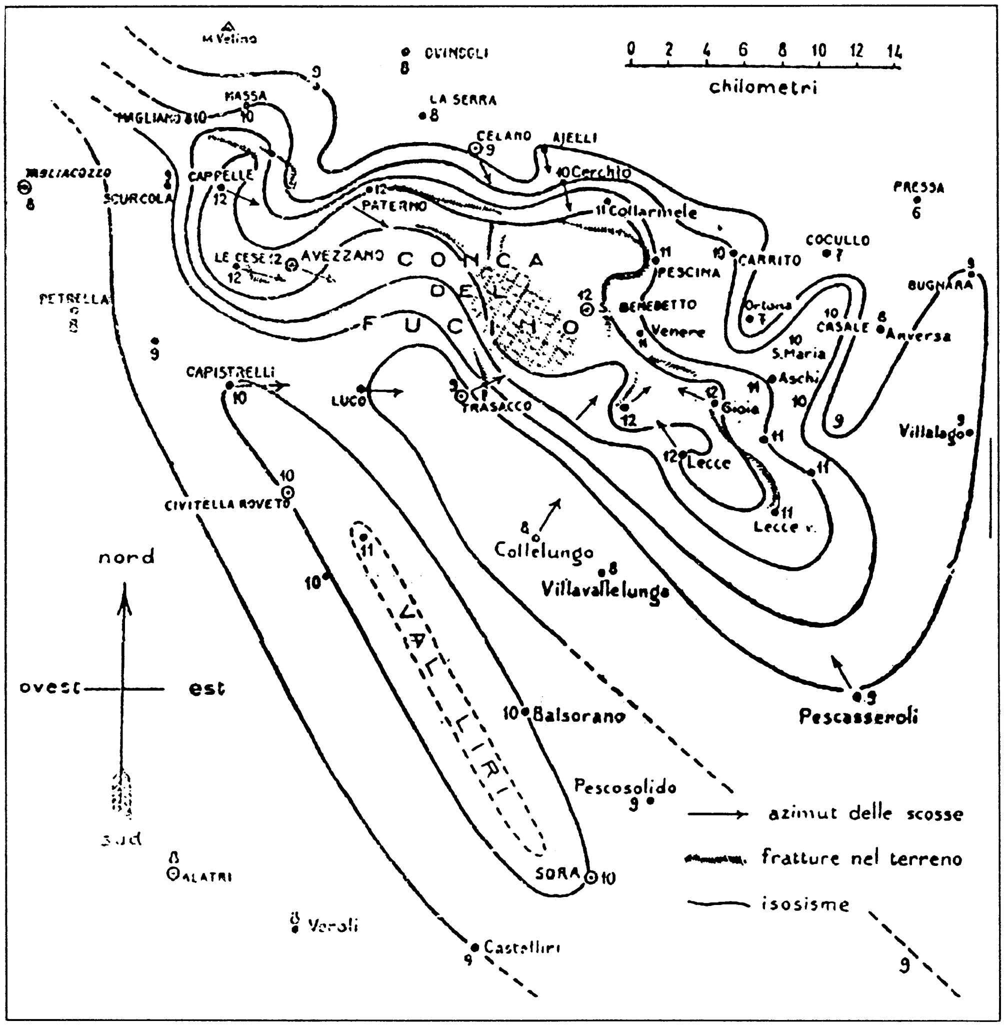

Fig. 5. Map of surface ruptures produced by the 1915 earthquake and damage distribution, from Oddone (1915). Arrows represent the direction of the seismic wave propagation; surface breaks and isoseismals are reported with hatched and black lines, respectively.

observations for possible faulting in the inner and western portions of the basin. In fact according to Oddone's report and other historical sources surface faulting may also be expected along the Trasacco fault (TF).

No clear evidence of the 1915 scarps are presently found along the MHF due to intense agricultural cultivation, and therefore reconstruction of the surface faulting pattern in the area between Cerchio and Pescina is based on the above-mentioned historical data. Precise field-based recognition of the rupture is therefore not possible, and the only certainty is that (according to historical sources) it was located at the base of the 70 m-high scarp which affects the middle Pleistocene deposits and landforms along the MHF.

In contrast, a retreated fault scarp affects the area between S. Benedetto dei Marsi and Venere along the SBGF, where historical reports locate the 1915 surface. This NW–SE trending scarp is about 0.5–0.7 m high and affects lacustrine sediments related to the last depositional phases of Lake Fucino along an approximately 3 km-long branch. As in the case of the MHF, more than 80 years of farming has made it very difficult to detect the scarp in the field, and only a preliminary survey of the oldest available aerial photographs (made by the R.A.F. in 1943) allowed the precise location of the rupture. The scarp appears to be very fresh on the R.A.F. photographs and therefore there is little doubt that it was formed as a result of the 1915 earthquake. A fault scarp about 5 km long and 3–4 m high is also present in the area between Venere and Gioia dei Marsi, affecting a Holocene lacustrine wave-cut terrace partly carved on the carbonate bedrock (Giraudi, 1988). Available paleoseismological data (Galadini et al., 1997) clearly indicate that part of this scarp (which is en-echelon with the previously described scarp, see Fig. 2) formed in 1915. Southeast of Gioia dei Marsi a bedrock fault scarp affects the southern slope of Mt. Serrone (dashed line in Fig. 2). Oddone (1915), Alfani (1915) and newspapers released immediately after the earthquake reported the occurrence of ruptures along this slope; the descriptions do not, however, allow to discriminate between tectonic and gravitational movements.

No scarps are related to the long-term activity of the Trasacco and Luco dei Marsi faults (TF and LMF, respectively, in Fig. 2), and these faults appear on aerial photographs as very faint NW–SE trending lineaments affecting the lowest areas of the basin (see Fig. 3 and sections below). No evidence of 1915-related activity is therefore available from the surface for these two branches.

One of the geologic effects of the 1915 event was the subsidence of the plain, as shown by the geodetic levelling made by Loperfido (1919). The benchmarks included nine monuments of the Virgin, eight pillars and one memorial stone, all placed along the shore of the lake in 1862 at the beginning of the most recent drainage works. The displacement measured in 1917 varied between $+5$ cm and -54 cm. The inversion of the geodetic data allowed Ward and Valensise (1989) and Amoruso et al. (1998) to infer that the 1915 earthquake fault is a SW dipping normal fault, bordering the eastern side of the basin in agreement with the surface observations.

4. Previous paleoseismological studies

Paleoseismological studies have been conducted since 1988 in the Fucino area.

On the basis of a geomorphological study, Giraudi (1988) inferred the age of some fault scarps located along the eastern (SBGF) and northern (TMF of Fig. 1) borders of the basin which were in good agreement with archaeologically determined collapse events that occurred in caves surrounding the Fucino area. Four different events were identified in the last 20,000 years: the oldest occurred approximately between 20,000 and 13,000 years B.P., the second between 5500 and 5000 years B.P., the third between 3500 and 3000 years B.P., and the most recent during the Middle Ages.

Michetti et al. (1996) collected data from two trenches excavated along the SBGF and recognised the effects of two paleoevents, the oldest having occurred between the 6th and 9th century (High Middle Ages Event) and the second between the 9th and 14th century (Low Middle Ages Event). Evidence for the latter event is questionable and will be discussed in a specific section below in the light of more recent paleoseismological data.

Coseismic effects related to a High Middle Ages Event were determined also by Galadini and Galli (1996) in a preliminary analysis of four trenches excavated at the intersection of the TF and a Roman drainage channel built in the 1st–2nd century A.D. (site 11 in Fig. 2). One of the trenches showed that displacement of the channel-fill sediments occurred in the second half of the 1st millennium A.D.

The data obtained through the extensive paleoseismological study of the Fucino Plain have been reported in Galadini et al. (1997), while specific observations along the TF (sites 7, 8, 9 and 11 in Fig. 2) are described in Galadini et al. (1996). An updated report of the basic paleoseismological data is in preparation. All the available data will be summarised in the next sections.

5. Paleoseismological analysis

5.1. Trench investigation and dating methods

As reported in the introduction, paleoseismology of the investigated area has been allowed by trenches excavated ad hoc across the major Holocene fault branches, quarries, long excavations dug for the laying of pipelines and the walls of the present drainage channels. Paleoseismological data have been obtained from sites 1–14 (Fig. 2) while sites 15 and 16 did not give any evidence for faulting affecting Late Pleistocene–Holocene deposits and site 17 is related to speleothem ruptures in a cave.

In the following sections we summarise the geological and paleoseismological data available for the different fault branches.

All laboratory dates (^{14}C and thermoluminescence) and sample site locations are reported in Table 1. Radiocarbon dating of samples collected from peat levels and paleosols, as well as lacustrine or colluvial organic silts and sands, was conducted at two different laboratories (ENEA – Bologna, and CRAD – Udine). To account for CO_2 variation in the atmosphere the laboratory ages were calibrated using a standard program (CALIB 3.0 by Stuiver and Reimer, 1993) which permits the calculation of ages up to 18,400 years B.P. (Table 2).

Thermoluminescence analysis was made by the Department of Physics at the University of Milan on pottery shards of different ages (since about 3000 B.C.) using the fine-grain technique (see Zimmermann, 1971).

In some cases archaeologists were able to obtain archaeological dates for pottery fragments by analysing the pottery grain, the form of the fragment, the thickness of the pottery and the characteristics of decorations.

When it was possible to compare the thermoluminescence dates obtained from the pottery with archaeological dates for the same fragments, the former method consistently gave younger dates and the difference between the two dating methods increased with the age of the pottery. For example, at site 6, thermoluminescence dating gave 833$\pm$213 B.C. on a pottery fragment dated at 1700–1200 B.C. by means

Table 1
Laboratory ages obtained by means of the radiocarbon (samples UD and BO) and thermoluminescence methods (on pottery shards, samples T)

Sample	Age, B.P.	Site
UD449	1,450 ± 100	4
UD437	3,390 ± 70	10
UD438	3,490 ± 70	10
UD440	3,760 ± 70	2
BO393	5,060 ± 90	12
UD452	5,340 ± 100	4
UD436	5,670 ± 90	13
BO387	6,170 ± 140	2
UD451	7,120 ± 120	4
UD433	8,660 ± 100	13
UD434	9,260 ± 100	13
UD455	9,730 ± 140	*
UD453	9,950 ± 140	*
UD450	10,400 ± 140	4
UD435	10,790 ± 110	8
UD439	10,990 ± 120	13
BO391	12,100 ± 50	8
BO332	19,100 ± 650	1
BO390	23,420 ± 280	8
UD441	27,230 ± 450	7
BO354	32,520 ± 500	5
T1	661 ± 46	5
T2	708 ± 59	5
T3	730 ± 56	5
T4	766 ± 100	5
T5	789 ± 78	5
T6	1,444 ± 142	2
T7	1,547 ± 142	2
T8	2,783 ± 213	5
T9	4,670 ± 430	5
–	14,180 ± 260	**

* Site not reported in Fig. 1 (west of and close to Bacinetto).
** Kieffer (1979) in reference to Mt. Etna and used for tephrachronology by Narcisi (1993).

Table 2
Laboratory and calibrated ages [a]

Sample	Laboratory age, B.P.	Calibrated age, B.C. (2σ)	Description
UD449	1,450 ± 100	426–782 (A.D.)	peat
UD440	3,760 ± 70	2,203–1,857	organic silt
BO393	5,060 ± 90	3,944–3,618	colluvium
UD452	5,340 ± 100	4,248–3,773	organic silt
UD436	5,670 ± 90	4,541–4,218	organic silt
BO387	6,170 ± 140	5,217–4,545	organic silt
UD451	7,120 ± 120	5,979–5,576	organic silt
UD433	8,660 ± 100	7,588–7,196	peat
UD434	9,260 ± 100	8,255–7,885	peat
UD455	9,730 ± 140	9,003–8,323	peat
UD453	9,950 ± 140	9,156–8,393	peat
UD450	10,400 ± 140	10,231–9,055	paleosol
UD435	10,790 ± 110	10,729–10,053	organic silt
UD439	10,990 ± 120	10,921–10,353	peat
BO391	12,100 ± 50	12,415–11,876	organic silt

[a] Calibration was made using a standard program (Stuiver and Reimer, 1993). Calibrated ages are reported in the text as calendar years A.D. and B.C. (limits of the 2σ interval derived from the probability distribution).

of archaeological analysis. At site 3, pottery fragments of the 1st–2nd century A.D. (archaeological analysis) were dated at 550 ± 147 A.D. and 447 ± 142 A.D. by means of thermoluminescence. In contrast, these dating problems do not affect another pottery fragment sampled at site 6, as thermoluminescence defined an age of 2720 ± 430 B.C. while archaeological analysis gave 2800–2600 B.C.

However, the investigated area is characterised by an abundance of archaeological sites which have been studied by means of stratigraphic archaeological criteria. For this reason, when dates are available both through thermoluminescence and through archaeologists' expertise, we consider the latter as the preferred age.

Some other chronological constraints were also derived, in particular for the inner and western portions of the basin, from the stratigraphic framework of the Late Pleistocene–Holocene lacustrine units (see geological framework section). Detailed stratigraphic correlations between the different studied sites were performed by surveys along drainage channels walls (representing an almost continuous network of exposures), surveys of the trench excavated for the aqueduct between Trasacco and Avezzano and by examination of a few hundred hand-boreholes. On these grounds it was possible to relate specific lacustrine units observed in the trenches across the TF and LMF to the stratigraphic columns reported in Fig. 4.

6. The main fault branches

6.1. The Marsicana Highway fault (MHF)

The Quaternary activity of the MHF (about 11 km long) is recorded by the displacement of Pliocene lacustrine sediments and Pleistocene fluvial and lacustrine sediments, with offset amount increasing with age. The fault is highlighted by a 70 m high scarp which affects Pliocene–middle Pleistocene fluvial deposits. These deposits and related terraces clearly appear to be suspended over the more recent deposits and the bottom of the historical lake (Fig. 6A). In line with the SE extent of the MHF, a minor fault branch along the SW slope of Mt. Parasano (Bosi et al., 1993; Blumetti et al., 1993) is highlighted by a continuous carbonate bedrock scarp (Fig. 6B).

As already pointed out, besides Oddone's mapping no direct geological evidence of the 1915 surface faulting or, more generally, of Holocene scarps can be recognised along this fault, probably due to the planation of the area related to intense agricultural work. The excavation of a long gas pipeline trench, which by chance crossed the MHF and a minor fault branch at sites 1 and 2, was therefore a unique possibility to collect paleoseismological data related to this fault.

At site 1 two fault planes (separated by 35 m) were observed affecting Late Pleistocene–Holocene deposits up to the level of the ploughed soil (Fig. 7). The pipeline trench crossed another fault at site 2. This site is exactly located on a ca. 1 km-long fault scarp (reported in Giraudi, 1988) which is parallel to the MHF. This scarp is interpreted as being the result of the activity of a minor fault branch, structurally related to the MHF.

The investigations at site 1 and, secondarily, at site 2 allowed the recognition of at least four displacement events which affected the MHF. The identified succession is represented by:

(1) an event, recorded at sites 1 and 2, which occurred after 2500 B.C. (this was likely the 1915 event, at least at site 1, considering that historical reports indicate ruptures in this area); the vertical offset at site 1 is 0.8 m, while at site 2 it is 1 m;

(2) an event which occurred between $19,100 \pm 650$ years B.P. and 2500 B.C. (recorded at site 1); the vertical offset related to this event is 0.36 m for the westernmost of the two faults at site 1, while a cumulative offset of 1.6 m can be calculated for the units affected by this and the subsequent events across the easternmost fault;

(3) another event which occurred between $19,100 \pm 650$ years B.P. and 2500 B.C. (recorded at site 1); a minimum total vertical offset can be calculated either for the westernmost fault (1 m), or for the easternmost one (2.2 m);

(4) one event which occurred approximately $19,100 \pm 650$ years B.P. (recorded at site 1); deposits affected by all the reported events (unit 7 in Fig. 7) have been found at the hanging wall of the westernmost fault and 150 m to the northeast of the easternmost one (with a horizontal attitude); it has

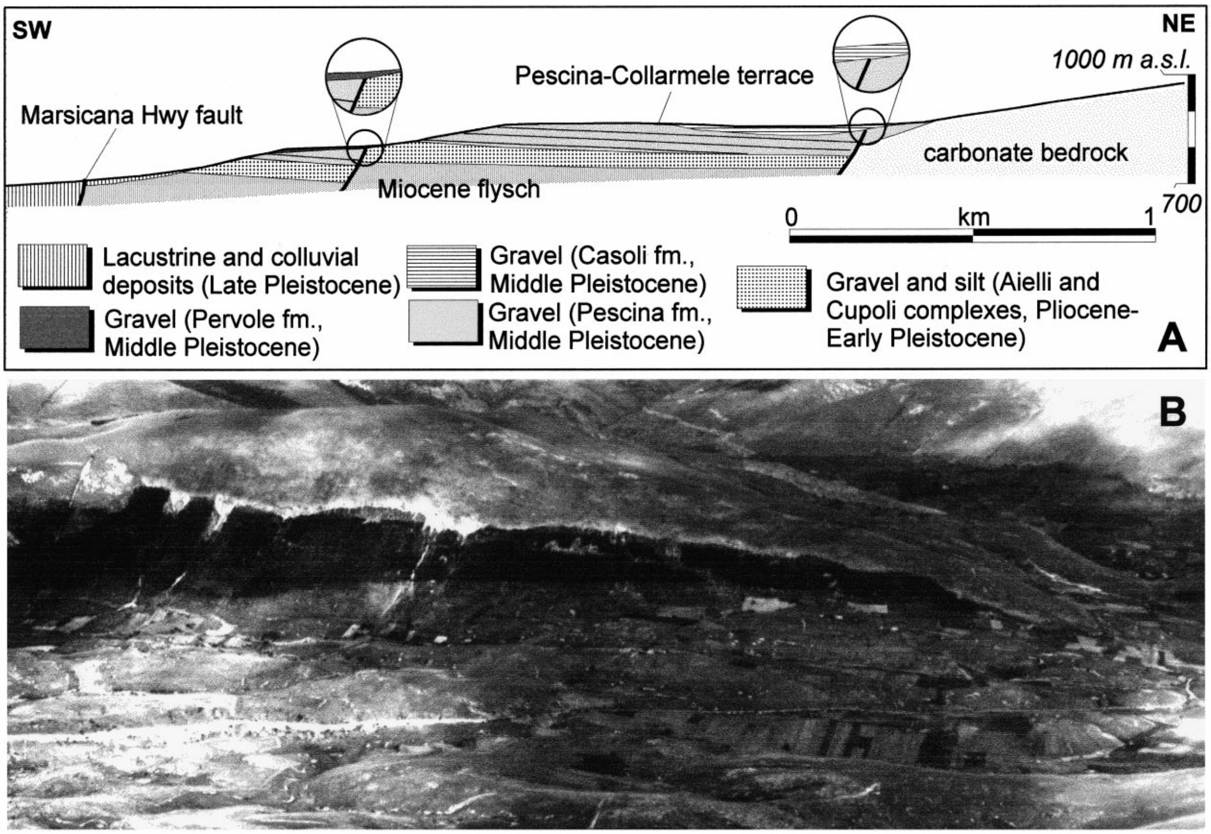

Fig. 6. Geological section (A) across the Marsicana Hwy fault (from Messina, 1996, modified) and aerial view (B) of the Mt. Parasano fault.

been possible to measure 7.5–9.5 m of vertical offset affecting this unit across the two faults.

6.2. The San Benedetto dei Marsi–Gioia dei Marsi fault (SBGF)

The activity along this fault branch was determined by analysing two trenches (sites 3 and 5) and two quarry exposures (sites 4 and 6).

The SBGF (about 12 km long) is composed by NW–SE trending fault scarps which affect a Late Pleistocene soft-rock pediment, a Holocene wave-cut terrace and the historical lacustrine deposits (Giraudi, 1988). The scarps usually occur in fluvial and lacustrine gravels or in lacustrine silts (Fig. 8A). In some places between Venere and Gioia dei Marsi, however, the Holocene wave-cut terrace is carved into the carbonate bedrock and the SBGF appears as a discontinuous, strongly weathered, few-metre-high carbonate bedrock scarp. Close to Casali d'Aschi the SBGF steps to the east (Fig. 2) and displaces Early and middle Pleistocene slope-derived breccias (Galadini and Messina, 1994). Southeast of Gioia dei Marsi the fault is easily detectable along the southern slope of Mt. Serrone (dashed line in Fig. 2) because it forms an impressive carbonate bedrock scarp (Fig. 8B). The fault plane is usually exposed along the scarp showing dip-slip kinematic indicators (mainly striae) and place the carbonate bedrock in contact with Late Pleistocene slope deposits.

In contrast to the MHF, the SBGF fault scarps are detectable on aerial photographs and recognisable in the field. This recognition become very difficult when the scarp affects silty lacustrine sediments, as at site 5 (Fig. 9), because the scarp is almost completely bevelled due to intense farming. In this case several 4-m-deep hand-boreholes were necessary to exactly define the position of the fault. The

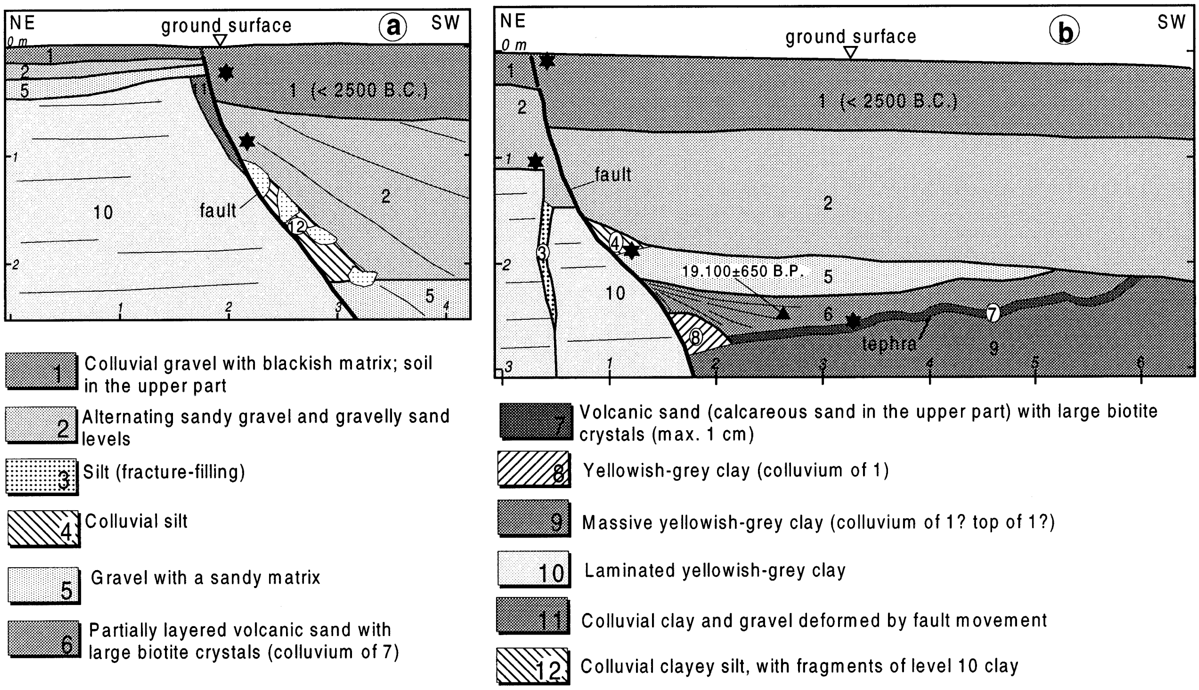

Fig. 7. Geological cross-sections of the gas pipeline trench at site 1 (southern wall). Section (b) is located 35 m to the west of section (a). Small stars indicate the event horizons; the triangle represents the sampling site. The older date is obtained by means of the radiocarbon method; unit 1 is a colluvium which buries an archaeological settlement close to this area, dated back to 2500 B.C.

hand-boreholes were dug 20–30 cm apart along lines perpendicular to, and crossing, the general trend of the SBGF (Galadini et al., 1995). In some cases the vertical displacement affecting sedimentary units was defined, based on the interpretation of the obtained sections.

The scarp is more easily recognisable at sites 3 and 4 because it affects the carbonate bedrock. The trench location at site 3 was identified without further surveys, while the southern wall of an abandoned quarry was logged at site 4 (located 20 m north of site 3).

Several quarries are present in the area close to Casali d'Aschi and many of them show displacements affecting slope deposits. In the quarry at site 6 it was possible to define a succession of displacement events and obtain chronological constraints for them. Analyses using aerial photographs and geomorphological surveys, however, showed that this area is clearly affected by deep-seated gravitational movements. This has been carefully considered in the interpretation of paleoearthquakes at this site.

On the basis of the analyses performed at sites 3, 4, 5 and 6 it is possible to summarise the succession of displacement events which have occurred along the SBGF:

(1) the 1915 event (at all sites); the offset related to this event ranges between 0.30 m (site 6) and more than 0.60 m (site 3);

(2) an event which occurred shortly after 426–782 A.D. (at all sites); the offset related to this event is larger than 0.30 m at site 3; deposits affected by this event and that which occurred in 1915 show a minimum total offset of 1.20 m at site 4; the 6 m vertical offset calculated at site 6 is the result of a gravitational component;

(3) an event contemporaneous with the deposition of sediments dated at 833 $\pm$ 213 B.C. using the thermoluminescence method, or at 1700–1300 B.C. with archaeological methods (site 6); the large value of vertical offset associated to this event at site 6 (1.5 m) is probably the result of a gravitational component;

(4) a probable event not much younger than 10,231–9055 B.C. and much older than 5979–5576

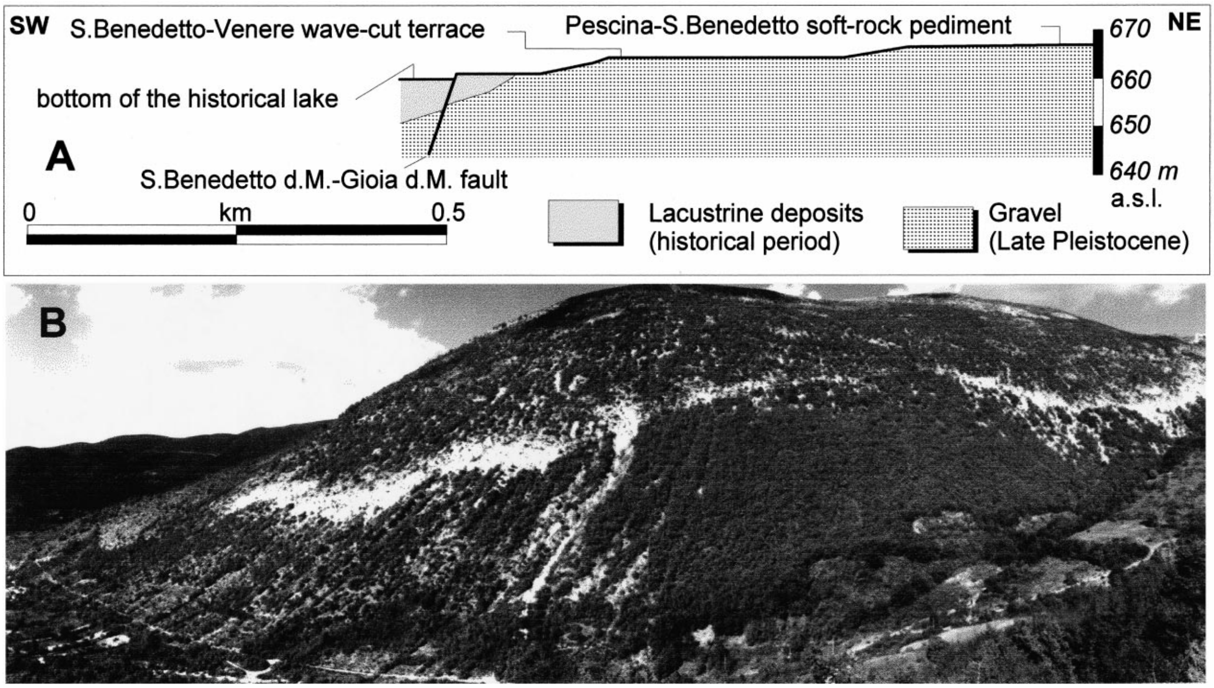

Fig. 8. Geological section (A) across the San Benedetto dei Marsi–Gioia dei Marsi fault (from Giraudi, 1988, modified) and aerial view (B) of the Mt. Serrone fault.

B.C. (site 5); the deposits affected by this and the more recent events at site 5 show a minimum total offset of 3 m;

(5) an event which occurred between 20,000 years B.P. and the limit Late Pleistocene–Holocene (site 6); the vertical offset is larger than 0.7 m;

(6) an event which occurred between $32,520 \pm 500$ years B.P. and about 20,000 years B.P. (site 6).

Evidence of displacement older than that occurred shortly after 426–782 A.D. has been observed at site 3, but because of the lack of correlative deposits across the fault zone they cannot be defined.

An event has been observed at site 6, occurred between the limit Late Pleistocene–Holocene and 2720 ± 430 B.C. which may be related or subsequent to the event observed at site 5 between 10,231–9055 B.C. and 5979–5576 B.C.

6.3. The Trasacco fault (TF)

This NW–SE trending, 7.5 km-long branch runs across the inner portion of the basin, i.e. the flat area that was occupied by the central part of the historical lake. No field-based geomorphological features can be directly attributed to the TF, and this branch is only visible on aerial photographs or satellite images as a straight lineament representing the sharp contact between soils with different lithologies and moisture contents (Fig. 3). Giraudi (1986) hypothesised historical activity for the TF because of the freshness of the lineament, as shown by the lack of sediments sealing the contact between different soils.

About 300 hand-boreholes were necessary to precisely locate the fault in the field. Boreholing could easily reach a depth of 4 m in the soft (silts and clays) lacustrine sediments of the inner part of the lake (Figs. 10 and 11). The boreholes, dug 20–30 cm apart along lines perpendicular to and across the TF, permitted in some cases the reconstruction of fault geometry and related offsets. In particular it was possible to define a fault plane dipping 60° to 70° towards the southwest and a displacement generally larger than 1 m affecting the top of complex D of Fig. 4. Sedimentary units related to the top of complex D are easily detectable through boreholing due to their typical yellowish colour.

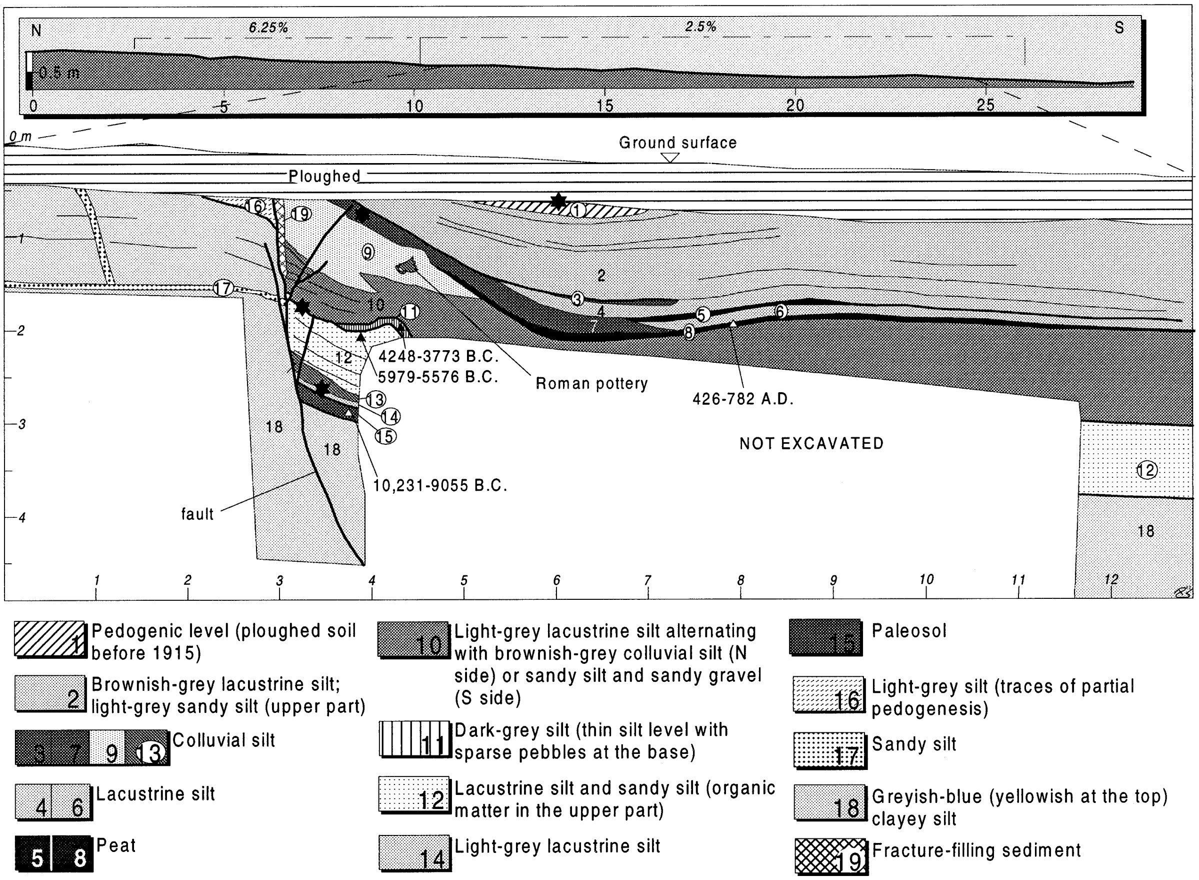

Fig. 9. Geological cross-section of the trench excavated at site 5 (S wall). Small stars indicate the event horizons.

On the basis of these preliminary surveys we selected sites 8, 9 and 11 (Fig. 2) as suitable for paleoseismological analysis. At site 11 the TF crosses the Roman drainage channel excavated in the 1st–2nd century A.D. Preliminary boreholing gave some evidence of the displacement of the channel bottom and trenching at this site was also performed because of the possibility to obtain precise chronological constraints about displacement events.

Further exposures are from a long, EW-trending trench excavated for the laying of an aqueduct that crossed the TF at site 7 (about 50 m north of site 8) and from site 10 which is located along the bank of one of the main drainage channels of the Fucino Plain (Fig. 2). The banks of the channels are usually covered by vegetation, but periodic cleaning is necessary to maintain the drainage system operational. Cleaning conducted at the beginning of 1996 allowed a paleoseismological analysis to be performed at this site.

Paleoseismological analysis allowed the identification of seven Holocene displacement events along the TF plus an older displacement event (which occurred approximately 15,666–14,397 B.C.) that was found only at site 11.

The Holocene events can be summarised as follows:

(1) the 1915 event (sites 7, 8, 9 and 11); the vertical offset ranges between 0.15 m (site 11) and 0.7 m (site 7);

(2) an event after or possibly during, the 5th–6th century A.D. (sites 7, 8, 9 and 11); the vertical offset ranges between 0.2 m (site 11) and more than 0.3 m (site 7);

(3) an event approximately during the 16th–15th century B.C. (sites 8, 11 and possibly 9); a mini-

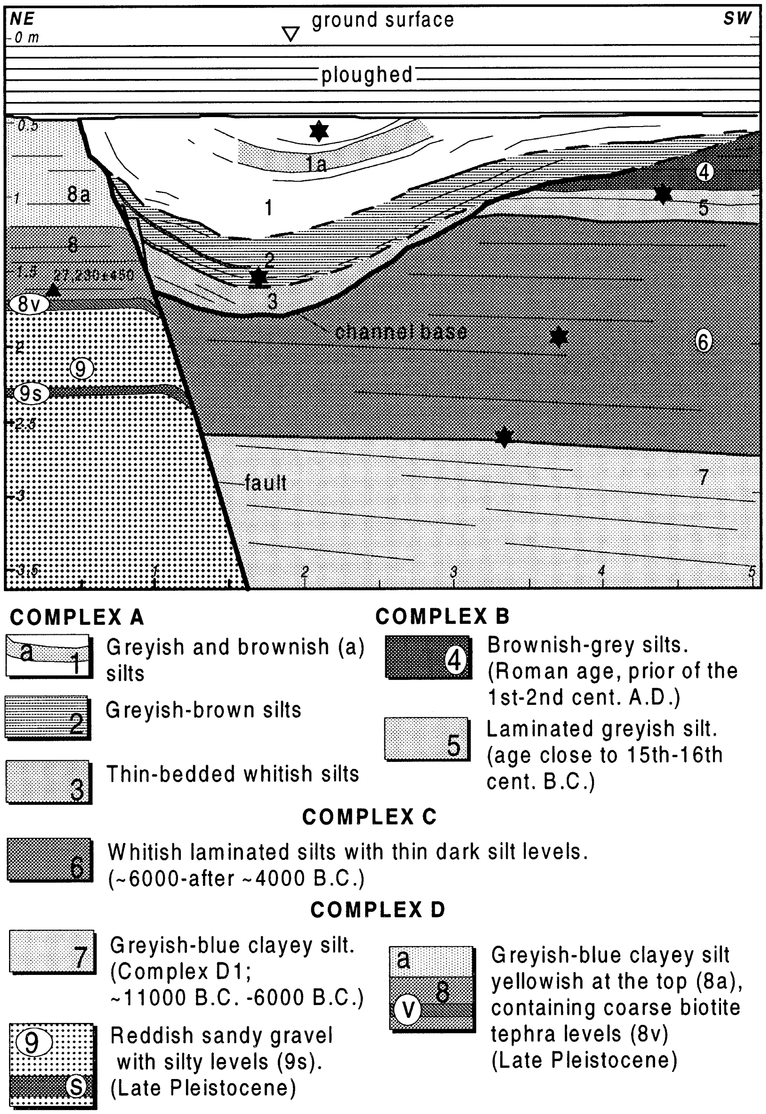

Fig. 10. Geological cross-section of the SE wall of the trench excavated at site 8. Small stars indicate the event horizons; the triangle represents the sampling site. The date is obtained by means of the radiocarbon method.

mum total offset of 0.7 m can be calculated for the sedimentary unit which was affected by this and the youngest events at site 8;

(4) an event which occurred about 3944–3618 B.C. (sites 9, 11, probably 10 and possibly 8); a minimum total vertical displacement can be calculated for the deposits affected by this and subsequent events at site 9 (0.9 m) and site 11 (0.6 m);

(5) an event more recent than 10,729–10,053 B.C. and preceding 5979–5576 B.C., possibly close to the latter date (sites 8, 9, 11 and probably 10); a minimum total vertical displacement can be calculated for the deposits affected by this and subsequent events at site 8 (3 m), site 9 (1.3 m) and site 11 (0.78 m);

(6) an event between 10,729–10,053 B.C. and 5979–5576 B.C. (sites 10 and 11); a minimum total vertical displacement can be calculated at site 11 (0.86 m);

(7) an event after 10,729–10,053 B.C. but close to this date (sites 9, probably 10 and possibly 11); the

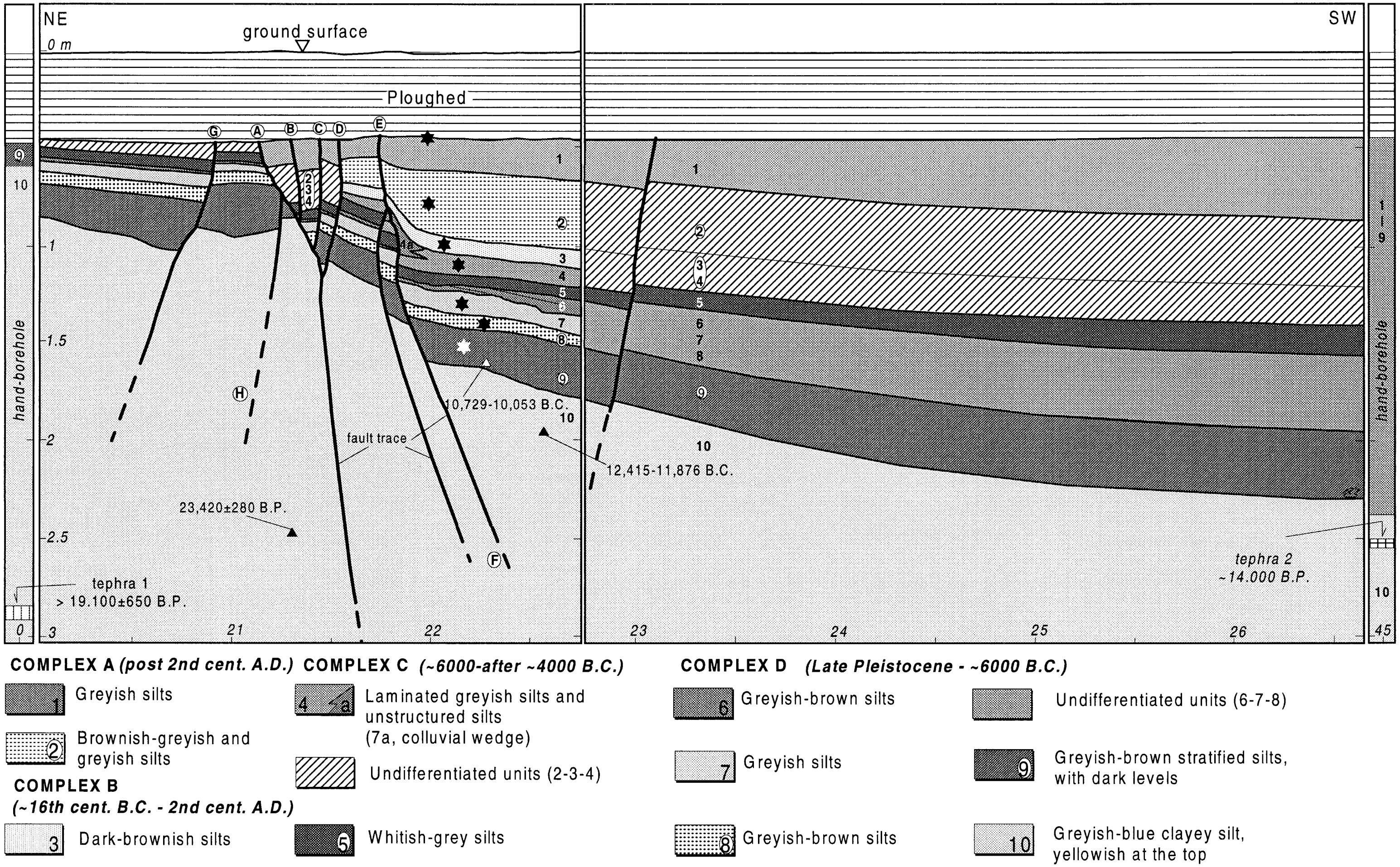

Fig. 11. Geological cross-section of the trench excavated at site 9 (SE wall). Small stars indicate the event horizons; triangles represent the sampling sites for radiocarbon analysis. Tephra 1 is one of the Late Pleistocene volcanic levels, the youngest of which has been found at site 1 and dated back at 19, 100 ± 650 years B.P. As for tephra 2, Narcisi (1993) related this level to an eruption of Mt. Etna (Sicily, southern Italy) which has been studied by Kieffer (1979) and which occurred about 14, 180 ± 260 years B.P.

minimum total vertical displacement is 1.8 m at site 9 and 1.2 m at site 10.

6.4. The Luco dei Marsi fault (LMF)

Like the TF, the ca. 4.5 km-long LMF is also visible on aerial photographs as a lineament due to the contact between soils with different lithologies and moisture contents. It was originally recognised by Giraudi (1986) for a length of about 1 km in the area close to the village of Luco dei Marsi. The investigation of the aqueduct walls, where it was expected to cross the LMF (see site 13 in Fig. 2), has revealed that this branch continues towards the north. Unfortunately, a very thick cover of reworked deposits is present at this site and thus the sedimentary succession which is suitable for paleoseismological analysis is only 1 m thick (Fig. 12).

The location of LMF and related displacement were also identified by digging hand-boreholes, augured perpendicular to a lineament which was observed on aerial photographs at site 12.

Analysis at site 12 only permitted to define 0.15 m of vertical offset affecting sediments deposited after the 4th century A.D. without distinction of displacement events.

Data obtained from site 13 allowed the identification of two displacement events, namely:

(1) the 1915 event, to which a vertical offset lower than 0.1–0.2 m is related;

(2) an event subsequent to the Roman drainage of the lake (1st–2nd century A.D.); the total vertical displacement related to this event and to the 1915 one across the investigated structure is 0.1–0.2 m.

6.5. The Tre Monti fault (TMF)

The TMF is a NE–SW trending, ca. 5 km-long branch of a longer fault which borders the northern sector of the Fucino basin, between Avezzano and the Aielli area. Galadini and Messina (1994) demonstrated, however, that the portion of the fault northeast of the basin has to be considered inactive, as it is sealed by middle Pleistocene slope-derived breccias. Since the middle Pleistocene the only active portion of this structure is thus the TMF, probably acting as a 'release fault' (sensu Destro, 1995).

The fault is located along the southern slope of the Tre Monti Mountain and appears at the surface as a carbonate bedrock fault scarp which consists of four main en-echelon segments. The TMF is responsible for the displacement of Pliocene lacustrine sediments

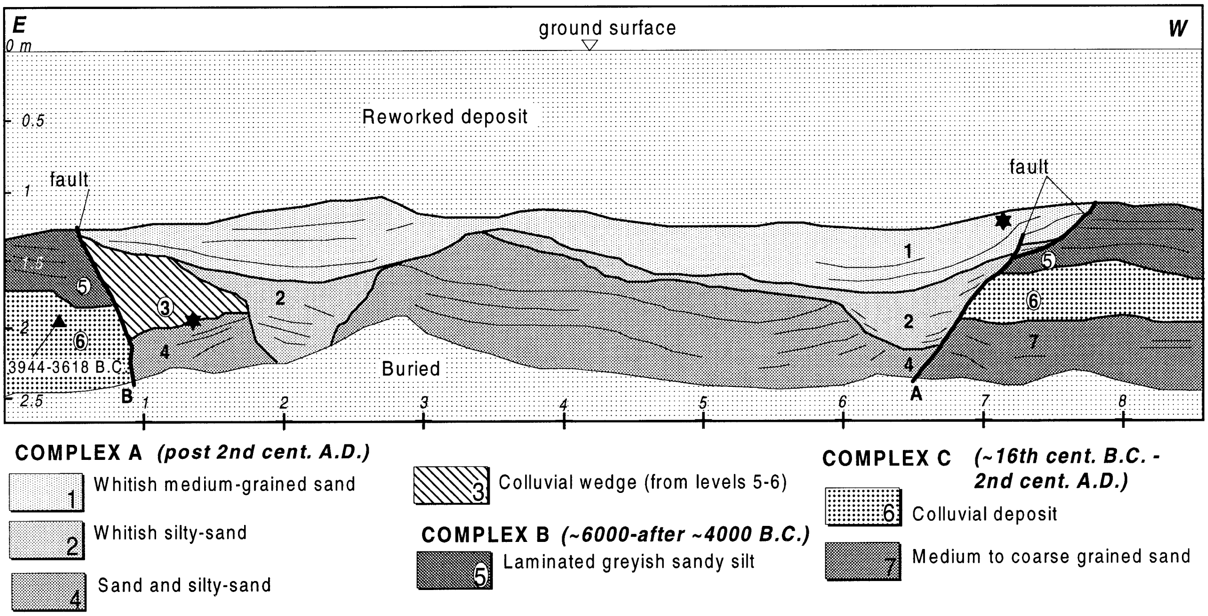

Fig. 12. Geological cross-section along the aqueduct trench (S wall) at site 13. Small stars indicate the event horizons.

and Pleistocene slope deposits. At the base of the slope affected by the fault some NE–SW fault scarps are present (up to 0.5 km long) which affect the depositional surface of Late Pleistocene gravels. The prolongation of these scarps towards the west-southwest coincide with an impressive scarp which affects the upper surface of a Late Pleistocene alluvial fan. Trenching and paleoseismological analysis performed on this feature (site 16) did not, however, show any evidence of faulting or other kind of deformation.

7. The paleoseismic events in the Fucino Plain

As already pointed out, the presence of a continuous Holocene sedimentary record in the inner part of the lake provided a unique opportunity to reconstruct the Holocene seismic history of the Fucino basin (in particular that of the TF), whereas only discontinuous information is available for the period between 32,000 years B.P. and the beginning of the Holocene.

As indicated in the geologic framework, the Fucino structure appears to consist of a primary fault system (SBGF–MHF) with secondary branches (TF and LMF). Movement along the latter faults has to be considered as the result of sympathetic slip accommodating part of the coseismic slip. Large-magnitude events originated from the primary fault system and were responsible for the activation of the entire Fucino structure.

Available paleoseismological data are summarised in Fig. 13 and Table 3. The different events

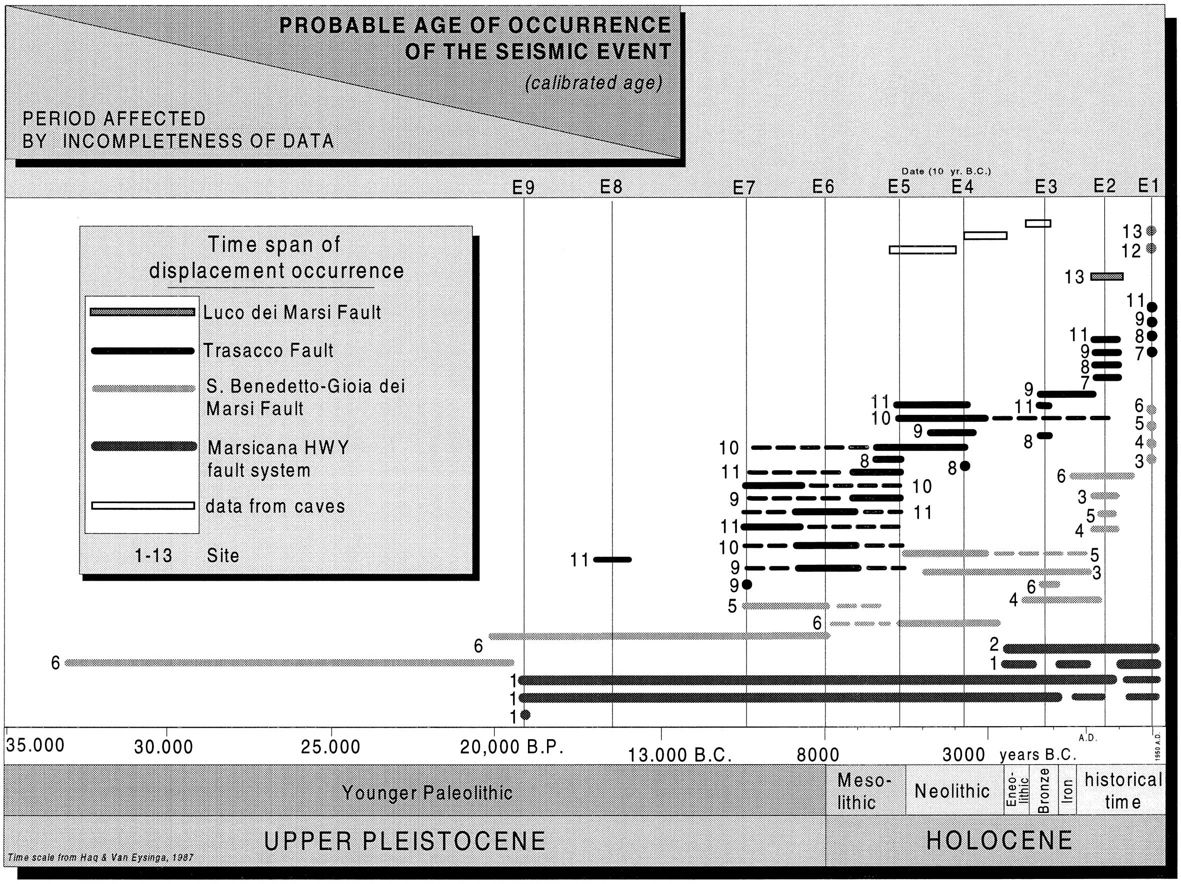

Fig. 13. Age ranges of the observed coseismic displacement events (recognised through the study of trench and quarry exposures and through the collapse of speleothems). The dashed part of the interval represents the less probable time span of occurrence. Numbers besides the segments indicate the studied sites (Fig. 2).

Table 3
Summary table of the Late Pleistocene–Holocene displacement events

Event	Age of displacement	Vertical offset	Fault	Site
E1	1915	>0.6	2	3
	1915	>0.3	2	4
	1915	~ 0.6	2	5
	1915	0.3	2	6
	1915	~ 0.7	3	7
	1915	>0.4	3	8
	1915	$>0.4^{\wedge}$	3	9
	1915	~ 0.15	3	11
	1915	<0.1–0.2	4	13
	1915	>0.3	–	14
E2	2nd–15th cent. A.D. (508 A.D.?)	>0.3	2	3
	2nd–15th cent. A.D. (508 A.D.?)	[>120]	2	4
	$\sim$426–782 A.D. (508 A.D.?)	–	2	5
	833 $\pm$ 213 B.C.–3th cent. A.D. (508 A.D.?)	0.2; 6 [6.5]	2	6
	2nd–15th cent. A.D. (508 A.D.?)	>0.3	3	7
	2nd–15th cent. A.D. (508 A.D.?)	>0.25	3	8
	2nd–15th cent. A.D. (508 A.D.?)	[>0.7]$^{\wedge}$	3	9
	2nd–15th cent. A.D. (508 A.D.?)	~ 0.2	3	11
	2nd–15th cent. A.D. (508 A.D.?)	[0.1–0.2]	4	13
E3	$\sim$833 $\pm$ 213 to 1300–1700 B.C.	0.15 [8]	2	6
	$\sim$15th–16th cent. B.C.	[>0.7]	3	8
	15th cent B.C.–2nd cent. A.D.	–	3	*9*
	$\sim$15th–16th cent. B.C.	–	3	11
E4	$\sim$*3944–3618 B.C.*	*[>2]*	3	*8*
	$\ll$5979–$\sim$3550 B.C.	[>0.9]$^{\wedge}$	3	9
	5979–$\sim$3550 B.C.	[>0.6]	3	11
E5	$\ll$10,729–5576 B.C.	[>3]	3	8
	10,729–5576 B.C.	[>1.3]	3	9
	10,729–5576 B.C.	[0.78]	3	11
E6	10,729–5576 B.C.	–	3	10
	10,729–5576 B.C.	[>0.86]	3	11
E7	*10,231$\gg$5576 B.C.*	*[>3]*	*2*	*5*
	$\sim$10,729–10,053 B.C.	[1.8]$^{\wedge}$	3	9
	10,729–5576 B.C.	[1.2]	3	10
	10,729–5576 B.C.	*[$\sim$1]*	*3*	*11*
Undefined	after 2nd cent. A.D.	~ 0.15	4	12
	after 19,100 $\pm$ 650 B.P.	[>2.2]* [>1]**	1	1
	after 19,100 $\pm$ 650 B.P.	[1.6]* 0.36**	1	1
	after 2500 B.C.	0.4* 0.4**	1	1
	after 2500 B.C.	[$\sim$1]	1	2
	5979 $\gg$ 2nd cent. B.C.	–	2	5
	20,000 B.P. to Holocene–L. Pleist. limit	>0.7	2	6
	$\ll$Holocene–L. Pleist. limit $\gg$ 2720 $\pm$ 430 B.C.	[10?]	2	6
	$\ll$10,729–10,053 to 3944–3618 B.C.	–	3	10
	after 5979–5576 B.C.	–	3	10
E8	$\sim$15,666–14,397 B.C.	–	3	11
E9	19,100 $\pm$ 650 B.P.	[7.5–9.5]	1	1
E10	$\sim$32,520 $\pm$ 500 to 20,000 B.P.	–	2	6

$\ll$ = age much younger than that reported; $\gg$ = age much older than that reported; $\sim$ = age close to that reported; $>$ = minimum offset that can be evaluated; [] = cumulative offset (including all the events between E_n and 1915); ˆ = total deformation (fragile plus continuous).
*, ** = site 1 (Fig. 7b), site 1 (Fig. 7a), respectively.
Italic points out low confidence events.

are reported in the text as E1 (the most recent) to E10 (the oldest).

7.1. The Holocene events

Seven displacement events are recorded during the Holocene.

The most recent displacement event (E1), which clearly ruptured all the studied faults, is related to the 1915 earthquake.

The penultimate displacement event (E2), detectable in most of the studied sites with the exception of sites 1, 2, 10, 12, occurred shortly after 426–782 A.D.; Michetti et al. (1996) assume that this event is the 801 A.D. earthquake, whereas Galadini and Galli (1996) hypothesise that it is either the 508 A.D. or the 618 A.D. earthquake reported in the catalogues of historical seismicity.

Based on archaeological dating the previous displacement (E3), clearly recognised at sites 6, 8 and 11, probably occurred close to the 16th–14th century B.C. E3 may also have been responsible for the collapse of caves between 1800 and 1100 B.C. (Radmilli, 1981).

Another event (E4), observed at sites 9, 11 and probably 10 along the TF, occurred about 3944–3618 B.C. This event may also have been responsible for the collapse of caves between 3500 and 2200 B.C. (Radmilli, 1981).

Three further displacement events (E5, E6 and E7) are recorded along the TF between 10,729–10,053 B.C. and 5979–5576 B.C. The E5 event, closer to the latter date and recorded at sites 8, 9, 11 and probably 10, may be the same as the one responsible for the ruptures of speleothems that occurred between 6000 and 4000 B.C. at the Continenza Cave (site 17 in Fig. 2; Giraudi and Frezzotti, 1998). The oldest Holocene event (E7) occurred about 10,729–10,053 B.C. and it is recorded at sites 9, 11 and probably 10.

The two oldest events at site 5 and the fourth event back at site 6 are chronologically overlapping within the E4–E7 succession of events and there is no basis to associate them to one or the other.

7.2. The Late Pleistocene events

The youngest Late Pleistocene event (E8) is recorded by a displacement which occurred about 15,666–14,397 B.C. at site 11, while an older event is recorded at site 1 which occurred about $19,100 \pm 650$ years B.P. (E9). The oldest displacement event (or group of events; E10) occurred between $32,520 \pm 500$ years B.P. and about 20,000 years B.P. (site 6).

8. Time span between events

The time spans between the five most recent displacement events are given in Table 4. The time spans vary from about 1400 (between E1 and E2 events) to 2100–2600 years (between E3 and E4).

It was not possible to define the time interval between the E5–E7 events, due to poor age constraints. Three events, however, did occur between about 10,500 B.C. and about 5500 B.C. and thus, assuming they occurred at equal time intervals, one can calculate an average recurrence interval of 2500 years.

Available time intervals (Table 4) highlight a quasi-periodic distribution of the surface faulting events during the Holocene.

9. Slip and extension rates

A vertical slip rate of 0.4–0.5 mm yr^{-1} can be calculated for the MHF at site 1 by considering the cumulative offset (7.5–9.5 m) across the two fault planes observed at this site and recorded by deposits dated at $19,100 \pm 650$ years B.P.

A lower value (0.24–0.29 mm yr^{-1}) was calculated for the SBGF by considering the vertical offset (3–3.3 m) which affects the top surface of unit 18 at site 5 (Fig. 9), whose age is close to 10,231–9055 B.C. This slip rate, however, represents a minimum value, because it was obtained by calculating the vertical offset separating the top of unit 18 at the southernmost portion of site 5 from that at the northernmost portion (Fig. 9). Considering that the upthrown side underwent erosion at this site, testified by the number of colluvial episodes which affect the downthrown side, it is clear that the actual vertical offset and related slip rate are larger than the above-reported values.

Unfortunately, only observations on single sites

Table 4
Time span between Holocene events [a]

	Age of consecutive events	Time span between events	Mean time span
E1	1915 A.D.		
		1400	
E2	508 A.D. (?)		
		1800–2000	1900
E3	1500–1300 B.C.		
		2100–2600	2350
E4	~3944–3618** B.C.		
		1600–2400	2000
E5	~5979–5576** B.C.		
		≤5000	
E6	10,729–10,053 to 5979–5576** B.C.		
		≤5000	
E7	~10,729–10,053** B.C.		

[a] Due to the poorly-defined age of E6, the time span between E5 and E6 and between E6 and E7 is reported as the maximum possible interval, i.e. that deriving from E6 being very close to E7 or very close to E5.
** Calibrated radiocarbon ages.

are available for the MHF and the SBGF, therefore nothing can be said regarding slip variability along the faults.

In contrast, the more extensive data collected along the TF infers that the slip rate varies along this fault branch. A minimum slip rate of 0.27–0.29 mm yr^{-1} was calculated at site 8 (Fig. 10) by considering the minimum vertical offset (about 2.2 m) which affects the top surface of unit 9 (dated at 5979–5576 B.C.). To the north, however, the slip rate decreases. At site 9 the vertical slip rate is 0.14–0.15 mm yr^{-1}, calculated on the basis of the vertical offset (1.76 m) which affects the top of unit 10, dated at approximately 10,729–10,053 B.C. (Fig. 11). The slip rate at site 10 is 0.09 mm yr^{-1}, calculated on the basis of the vertical offset (1.13 m) which affects the same unit mentioned for site 9. This unit is affected by a vertical offset of 1 m at site 11, for which a slip rate of 0.08 mm yr^{-1} is calculated. This trend is probably related to the increasing depth of the carbonate bedrock below the plain from south to north, resulting in a kind of 'absorption' of vertical movement due to the presence of unconsolidated sediments (see Bray et al., 1994). If this is true, the most realistic measure of the slip rate for the TF is that calculated at site 8.

In regard to the LF, vertical offset data have been collected at site 13, where the surface separating units 5 and 6 is displaced by 0.1–0.2 m across the two faults detected at this site (Fig. 12). Considering that this surface formed not much after 3944–3618 B.C., the slip rate ranges between 0.017 and 0.036 mm yr^{-1}. However, considering that the paleoseismic record for the LMF only covers a short time span and that only one trench is available for this structure, this value is not considered completely reliable.

On the basis of the slip rate data collected at different sites along the four fault branches, it is possible to hypothesise the extension rate across the entire Fucino structure by summing the contribution of each investigated fault branch. A crucial point is represented by the variable dip caused by listric fault geometry (e.g. Mostardini and Merlini, 1986). Observed faults generally dip 60º towards the southwest at the surface, while their dip at depth is much lower. Amoruso et al. (1998) calculated a dip of 55º ± 10º for the seismogenic fault responsible for the 1915 earthquake by re-evaluating available seismological and geodetic data. Therefore, considering fault dip values between 45º and 60º, the total extension rate ranges across the whole Fucino basin between 0.6 and 1 mm yr^{-1}.

This may be a minimum value, however, considering that it was obtained using the vertical slip observed at the surface and that this value may be lower than the average subsurface slip (i.e. Wells and Coppersmith, 1994).

10. Discussion

10.1. The 1915 coseismic faulting

The investigations conducted in the Fucino area yielded a reconstruction of the surface faulting pattern produced by the 1915 event more complete than that available from previous works (e.g. Serva et al., 1986). In addition to the MHF and SBGF (whose slip is also suggested by Oddone's map), slip occurred also along the TF and LMF (Figs. 2 and 14).

Some unpublished historical data point to the formation of scarps along the TF (e.g. Saladino, 1915 in Galadini et al., 1995). However, 1915 slip along the TF and LMF is inferred from:

(1) displacement of the ploughed soil after the most recent drainage of the lake (site 7; Galadini et al., 1996);

(2) displacement of the most recent lacustrine sediments deposited just prior to the 19th drainage of the lake (complex A in Fig. 4) in areas (sites 8, 12 and 13; Galadini et al., 1996, 1997) which were submerged by the lake only during the last few centuries of this millennium;

(3) thickening of the ploughed soil across the TF (site 11; Galadini and Galli, 1996).

Unfortunately no geological data are available on the northern sector of the basin, along the TMF (Fig. 1), even though historical data (Alfani, 1915) point to the possible occurrence of surface faulting in 1915.

In short, on the basis of paleoseismological data, the fault branches reported in Fig. 2 represent the best available picture of the 1915 surface faulting. Fig. 14 highlights the surface slip distribution, that shows a decreasing vertical offset along the TF to-

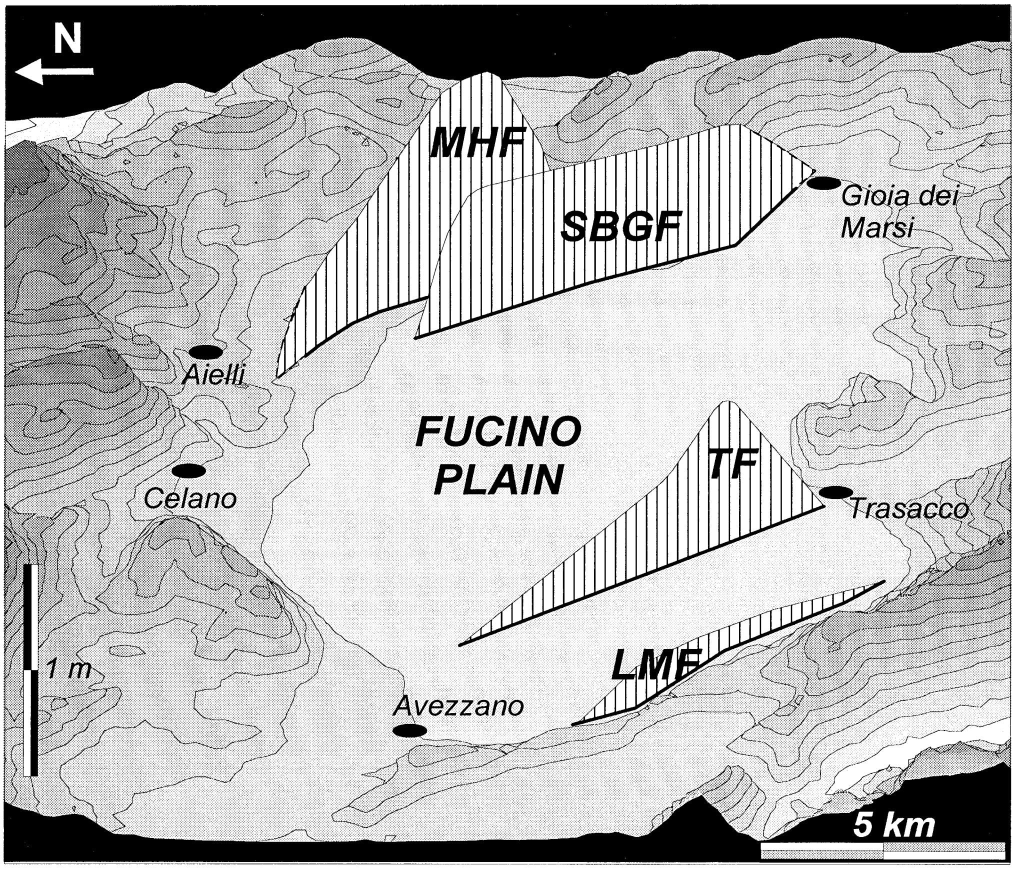

Fig. 14. 1915 vertical offset along the different fault branches (for quantification see the vertical bar).

wards the north and the en-echelon relationship between the SBGF and MHF.

10.2. One more earthquake during the Middle Ages?

Michetti et al. (1996) interpreted the attitude of some sedimentary units in their two trenches across the SBGF as being the result of deposition on a paleoscarp formed by erosion along a paleoshoreline or by coseismic movement of the fault. Due to the lack of shoreline deposits, the authors preferred the second hypothesis and related the deposit to a surface faulting event that occurred during the Low Middle Ages (LMAE). The authors hypothesise that the LMAE may be the 1349 event, even though the damage distribution of this earthquake does not seem consistent with an origin in the Fucino area (e.g. Boschi et al., 1995).

In contrast, we have not found any trace of the LMAE at the different sites we analysed. At site 5, which is located along the same branch investigated by Michetti et al. (1996), we found many sedimentary episodes and erosive traces related to the evolution of the lacustrine shoreline, similar to the exposure of Michetti et al. (1996). Therefore, we prefer the paleoshoreline erosion hypothesis and following a conservative approach we conclude that a LMAE did not originate, nor produced surface faulting, in the Fucino basin.

10.3. The Fucino fault and adjacent structures

Galadini and Messina (1994) defined a main active structure in this sector of the Apennine chain, represented by a 80 km-long lineament consisting of en-echelon branches located between the upper Sangro River valley and the town of L'Aquila. The Fucino fault lies in the central part of this zone and its prolongation towards the north is represented by the Ovindoli-Pezza and Campo Felice faults (OPF and CFF, in Fig. 1), while the southern prolongation is represented by the Sangro Valley fault zone and the Pescasseroli fault (SVFZ and PF in Fig. 1).

A paleoseismological study conducted along the OPF by Pantosti et al. (1996) found the traces of three displacement events: the oldest occurred between 5000 and 3300 B.C.; the penultimate about 1900 B.C.; and the most recent between 860 and 1300 A.D. The recurrence interval between the last two events ranges between 2760 and 3200 years. These data suggest that although the OPF and the Fucino faults are adjacent and they slip at similar rates, the timing of their events is completely independent. Therefore, in the time period investigated there is neither evidence of 'cascading' rupture of the OPF and Fucino fault, nor evidence of synchronous activation responsible for larger-magnitude events.

Similarly, recent investigations carried out by Giraudi (1995) in the Campo Felice area (Fig. 1) show that the most recent slip event along some faults connected with the CFF probably occurred in the last 2500–3000 years.

The fault branches of the upper Sangro River valley (SVFZ and PF in Fig. 1) are also in-line with the SBGF. Published data only indicate post-Early Pleistocene activity (Galadini and Messina, 1993); more recent data (Galadini et al., 1999), however, highlight a post-26,000 years B.P. activity of the PF. Recent activity in this area is confirmed by geomorphological evidence such as the fresh fault scarp affecting Early Pleistocene gravels along most of the PF. In addition, data on active tectonics are available for a sector of the Sangro Valley, southeast of that reported in Fig. 1, where deposits of glacial origin related to the last glacial maximum are clearly faulted (Giraudi, 1995).

However, evidence of strong ($M > 6$) historical earthquakes are lacking in the Sangro Valley and therefore it appears necessary to address future research at collecting paleoseismological data in this sector of the Apennine chain.

10.4. Comparing the paleoseismological results and the historical record

Recent paleoseismological research in the Apennine chain shows that the recurrence intervals of displacement events usually range between more than 1000 and 3000 years (Pantosti et al., 1993, 1996; Giraudi and Frezzotti, 1995; Cinti et al., 1997). Data regarding the time span between the surface faulting events in the Fucino Plain are completely consistent with this trend and show that the behaviour of the Apennine seismogenic structures responsible for surface faulting events is characterised by long recurrence intervals.

The historical record of earthquakes in Italy covers a time interval of more than 2000 years (Boschi et al., 1997), although it is obviously less complete with regards to older events. A comparison of the length of recurrence intervals of strong events and the time span covered by the Italian seismic catalogues reveals that the latter do not necessarily include records of all the Apennine seismogenic structures. This observation, already stated by other authors (e.g. Pantosti et al., 1996), is also highlighted by the fact that geologic data in the Apennines show the presence of active faults that, according to historical records, did not rupture during the time interval covered by the catalogues (examples are the Ovindoli-Pezza fault, studied by Pantosti et al., 1996, and the Sangro Valley fault zone, both mentioned in the previous section).

10.5. Extension rates and active fault sets in the central Apennines

The extension rate through the Fucino Plain (0.6–1 mm yr^{-1}) is consistent with that evaluated by Pantosti et al. (1996) for the Ovindoli-Pezza fault, north of the investigated area (0.4–1.1 mm yr^{-1}). These are the only direct data available from the central Apennines which can be used to discuss the seismic extension rate across this Apennine sector.

The geologically inferred extension has been compared with that obtained by summing the seismic moments of the historical earthquakes which occurred in an area including the Fucino seismogenetic structure. This approach is based on the equation:

$$v_s = \mathrm{Mo}/2\mu H L t$$

derived from Kostrov (1974), where v_s is the velocity of separation between two zone boundaries, Mo is the sum of scalar seismic moments, μ is the rigidity modulus, H the thickness of the brittle layer, L the length of the considered region, and t the time span covered by the catalogue. Since the extensional eigenvector (sensu Kostrov, 1974) of the seismic moment tensor is not subhorizontal for normal faults with dip $d \neq 45°$, according to Westaway (1992) the resulting relative velocity can be estimated as:

$$v_s = \mathrm{Mo}\ \sin(2d)/2\mu H L t$$

The magnitude values necessary for the evaluation of Mo have been taken from the two most recent available Italian catalogues (Boschi et al., 1997; Camassi and Stucchi, 1997, 1998) and the seismic moments have been calculated for the earthquakes falling inside the polygon reported in Fig. 15. The chosen area represents a part of the Apennines which is characterised by NW–SE normal and normal-oblique faults and related NE–SW extension.

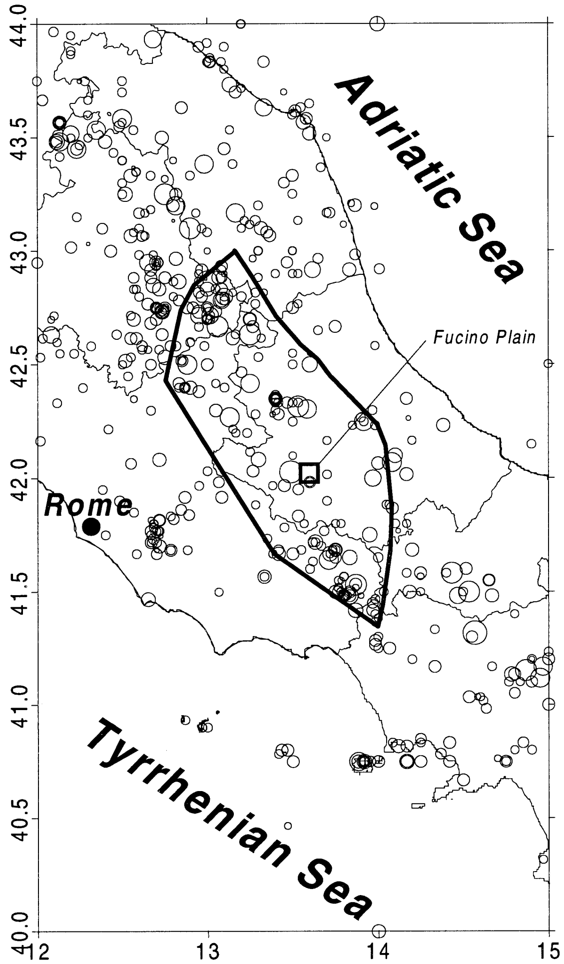

Fig. 15. Seismicity of central Italy (1000–1992, according to Camassi and Stucchi, 1997, 1998). The bold line delimitates the area selected for the evaluation of the extension rate through the summation of the seismic moment tensor.

Assuming $m = 3 \times 10^{11}$ dyn/cm^2, $H = 15$ km and $L = 150$ km, and considering fault dips ranging between 60° and 45°, the obtained seismic strain for the period 1000–1992 is between 0.8 mm yr^{-1} and 1 mm yr^{-1} using the catalogue by Camassi and Stucchi (1997, 1998) and between 0.5 mm yr^{-1} and 0.6 mm

yr^{-1} using the catalogue by Boschi et al. (1997). The discrepancy between the obtained seismic strain values is due to the fact that the magnitudes reported in the former catalogue are generally larger than those reported in the latter.

However, the choice of the period may affect the results. In fact, historical information is not homogeneous throughout the entire interval 1000–1992, being more scarce in the early centuries.

More homogeneous information is available for earthquakes with $M \geq 6$ (whose contribution to the total seismic moment is greater than 90%) in the period 1300–1992. With this time interval, the extension rate is 0.9–1.1 mm yr^{-1} considering the catalogue by Camassi and Stucchi (1997, 1998) and 0.7–0.9 mm yr^{-1} considering the catalogue by Boschi et al. (1997).

The obtained values are similar to the paleoseismologically inferred rate throughout the Fucino structure (0.6–1 mm yr^{-1}). However, at least another active and seismogenic fault system affects the central Apennines, paralleling the Fucino structure to the east (i.e. the Sulmona-Gran Sasso fault system; e.g. Vittori et al., 1995; Giraudi and Frezzotti, 1995). Therefore, the similarity between the differently calculated extension rates points to a seismicity 'deficit' in the central Apennines during the last millennium. This is consistent with the conclusion of the previous section, indicating that a number of active faults in the central Apennines were not active during the past 1000 years.

10.6. Faulting behaviour of the Fucino seismogenic structure

Offset-per-event data related to the primary faults of the Fucino basin (the MHF and SBGF) are lacking. However, an evaluation of the MHF slip rate (0.4–0.5 mm yr^{-1}) is available at site 1, along with evidence related to vertical offset caused by the 1915 event. In fact, on the basis of historical data which indicates that about 0.9 m of displacement (divided into two adjacent scarps with comparable vertical offset) occurred in 1915 close to site 1, it is conceivable that the displacement of about 0.8 m observed in unit 1 (due to both faults detected at this site) is entirely related to the 1915 event. Considering the age of unit 7 (about 20,000 years B.P.) and the average time interval for the Fucino events (about 1900 years), one finds that unit 7 was probably affected by ten events. If the fault has a characteristic behaviour, the 0.8 m displacement observed at this site due to the 1915 event would yield a total displacement of about 8 m. This is comparable to the total offset of 7.5–9.5 m observed at site 1.

Another interesting point is obtained by comparing the offset affecting units 1 and 2 along the westernmost fault detected at site 1 (Fig. 7b). On the basis of historical data, the 0.4 m displacement affecting unit 1 may be entirely related to the 1915 event, while the offset due to the previous event is 0.36 m. The similarity of the offsets produced by these two events, as well as evidence given by the comparison of long-term slip rates and the slip data related to the 1915 earthquake, may indicate a constant 'displacement-per-event' over time.

Unfortunately, site 1 is the only site along the MHF, and thus there are no other data which can confirm the characteristic behaviour of the Fucino fault. In fact, as pointed out in the previous section, the vertical slip rate evaluated for the SBGF at site 5 (0.24–0.29 mm yr^{-1}) represents a minimum value, and therefore reliable results cannot be expected from a comparison of the 1915 offset with the long-term slip rate. However, historical data at site 5 indicates that 0.6 m of vertical displacement occurred in 1915. Deposits dated at 10,231–9055 B.C., which may have suffered all seven Holocene events in the Fucino basin, are displaced 3–3.3 m; this is about 1 m less than that expected for characteristic behaviour and assuming 0.6 m as characteristic slip.

At sites 3 and 4 only minimum values for the 1915 offsets may be considered along the SBGF; moreover, the evaluation of the slip rate at these sites may be unreliable due to the unknown depositional geometries of the sedimentary units affected by the fault. In addition, the displacements observed at site 6 appear to be clearly affected by gravitational components.

Vertical offset data and slip rates are available for sites 9 (0.14–0.15 mm yr^{-1}), 10 (0.09 mm yr^{-1}) and 11 (0.08 mm yr^{-1}) along the TF, while a minimum slip rate is available for site 8 (0.27–0.29 mm yr^{-1}). Available data show that an almost constant displacement-per-event may affect the fault branch in the inner sector of the basin. However, as the TF is a secondary fault, these data are inconclusive for the assessment of seismogenic structure behaviour.

In short, the only reliable data related to the seismogenic behaviour of the Fucino fault were obtained along the MHF at site 1. These data may infer a characteristic behaviour of the fault, but the lack of other sites with similar results means that conclusive hypotheses cannot be presented.

11. Conclusions

The paleoseismological research conducted in the epicentral area of the 1915 Avezzano earthquake ($M_s = 7.0$), represents the final step of a detailed geological and structural study aimed at defining the Holocene faulting pattern and Late Pleistocene–Holocene geological evolution of the region (Giraudi, 1988; Galadini and Messina, 1994; Galadini et al., 1995). Through the study of trench walls and exposures and the analysis of collected data it was possible to:

(1) reconstruct that the surface faulting pattern of the 1915 event is due to slip on four different fault branches over a 15 km $\times$ 20 km large area;

(2) identify the displacements due to ten seismic events which occurred since $32,520 \pm 500$ years B.P., seven of which occurred during the Holocene;

(3) define a recurrence interval for events responsible for surface faulting which ranges between 1400 and 2100–2600 years (average 1900 years);

(4) calculate a slip rate of 0.4–0.5 mm yr^{-1} for the MHF and minimum slip rates of 0.24–0.29 mm yr^{-1} and 0.27–0.29 mm yr^{-1} for the SBGF and the TF, respectively, as well as an extension rate across the Fucino Plain between 0.6 and 1 mm yr^{-1};

(5) determine the quasi-periodic distribution of surface faulting events over the Holocene.

Data on the Fucino area are consistent with recently published paleoseismological works on active faults of the central Apennines (e.g. Pantosti et al., 1996). Moreover, these data improve our understanding of the seismogenic processes in this sector of the Apennine chain, characterised by faults with slip rates lower than 1 mm yr^{-1} responsible for large earthquakes ($M \geq 6.5$) each 1000–2000 years.

The comparison between the Fucino paleoseismological data and the paleoseismological data set related to the Ovindoli-Pezza fault (north of the Fucino Plain; Pantosti et al., 1996) shows no apparent chronological relationship between the events that occurred along the two faults, due to the different recurrence time of surface faulting events. In contrast, neither paleoseismological nor historical data on $M > 6$ earthquakes are available for the southern prolongation of the Fucino structure (i.e. the Sangro Valley fault zone), despite geomorphological evidence of the present tectonic activity.

Another implication derives from the similarity of the extension rate (paleoseismologically inferred) across the Fucino Plain and that obtained by the summation of seismic moments related to historical earthquakes in the period 1000–1992, throughout the entire central Apennines. Since at least two parallel systems of active faults affect the central Apennines, the similarity of the differently calculated extension rates indicates that a number of faults were not active since 1000 AD. This is not anomalous, considering that the time span between two large events related to an Apennine fault is usually larger than 1000 years. A general consequence (already stated by other authors, such as Pantosti et al., 1996) is that the Italian seismic catalogues appear to be insufficient to record all the latest events caused by the different seismogenic structures affecting the Apennine chain, despite the long time period covered by historical information. As a result the activity of many faults may not be reported in the seismic catalogues and, paradoxically, may have a major impact on seismic hazard assessment (due to the lack of events in the last 1000 years). This observation clearly directs future geological and paleoseismological research towards the individuation and characterization of historically 'silent' active faults.

Acknowledgements

We are grateful to M. Meghraoui and D. Pantosti for helpful discussions; their review of the manuscript has greatly improved it.

References

Alfani, G., 1915. Appunti di viaggio del Padre G. Alfani sui luoghi maggiormente danneggiati dal terremoto del 13 gen-

naio 1915. Manuscript of the Osservatorio Ximeniano archive, Firenze, 14 pp.
Amoruso, A., Crescentini, L., Scarpa, R., 1998. Inversion of source parameters from near and far field observations: an application to the 1915 Fucino earthquake, central Apennines, Italy. J. Geophys. Res. 103, 29989–29999.
Basili, A., Valensise, G., 1991. Contributo alla caratterizzazione della sismicità dell'area marsico-fucense. In: Boschi, E., Dragoni, M. (Eds.), Aree sismogenetiche e rischio sismico in Italia. ING, Rome, pp. 197–214.
Blumetti, A.M., Dramis, F., Michetti, A.M., 1993. Fault-generated mountain fronts in the Central Apennines (Central Italy): geomorphological features and seismotectonic implications. Earth Surf. Process. Landf. 18, 203–223.
Boschi, E., Ferrari, G., Gasperini, P., Guidoboni, E., Smriglio, G., Valensise, G., 1995. Catalogo dei forti terremoti in Italia dal 461 a.C. al 1980. Istituto Nazionale di Geofisica, SGA storia geofisica ambiente, Bologna, 973 pp.
Boschi, E., Guidoboni, E., Ferrari, G., Valensise, G., Gasperini, P., 1997. Catalogo dei forti terremoti in Italia dal 461 a.C. al 1990. Istituto Nazionale di Geofisica, SGA storia geofisica ambiente, Bologna, 644 pp.
Bosi, C., 1975. Osservazioni preliminari su faglie probabilmente attive nell'Appennino centrale. Boll. Soc. Geol. Ital. 94, 827–859.
Bosi, C., Galadini, F., Messina, P., 1993. Neotectonic significance of bedrock fault scarps: case studies from the Lazio-Abruzzi Apennines (central Italy). Z. Geomorphol. Suppl. 94, 187–206.
Bray, J.D., Seed, R.B., Cluff, L.S., Seed, H.B., 1994. Earthquake fault rupture propagation through soil. J. Geotech. Eng. 120, 543–561.
Camassi, R., Stucchi, M., 1997. NT4.1 a parametric catalogue of damaging earthquakes in the Italian area. Gruppo Nazionale per la Difesa dai Terremoti, Milano.
Camassi, R., Stucchi, M., 1998. NT4.1.1.1, file di aggiunta 81–92. Internet, http://emidius.itim.mi.cnr.it/NT/home.html
Carrara, C., Dai Pra, G., Giraudi, C., 1995. Lineamenti di tettonica plio-quaternaria dell'area. In: Lazio meridionale, sintesi delle ricerche geologiche multidisciplinari. ENEA, Dipartimento Ambiente, Bologna, pp. 151–155.
Chiarini, E., Messina, P., Papasodaro, F., 1997. Evoluzione geologica e tettonica plio-quaternaria dell'alta valle del F. Salto (Italia centrale). Primi risultati derivanti dall'analisi delle superfici relitte e dei depositi continentali. Il Quaternario 10, 625–630.
Cinti, F.R., Cucci, L., Pantosti, D., D'Addezio, G., Meghraoui, M., 1997. A major seismogenic fault in a 'silent area': the Castrovillari fault (southern Apennines, Italy). Geophys. J. Int. 130, 595–605.
CNR-PFG, 1983. Structural Model of Italy and Gravity Map. Quad. Ric. Sci. 114.
Destro, N., 1995. Release fault: a variety of cross fault in linked extensional fault systems in the Sergipe-Alagoas Basin, NE Brazil. J. Struct. Geol. 17, 615–629.
Galadini, F., Galli, P., 1996. Paleoseismology related to deformed archaeological remains in the Fucino Plain, implications for subrecent seismicity in central Italy. Ann. Geofis. 39, 925–940.
Galadini, F., Messina, P., 1993. Characterization of the recent tectonics of the upper Sangro River valley (Abruzzi Apennine, Central Italy). Ann. Geofis. 36, 277–285.
Galadini, F., Messina, P., 1994. Plio-Quaternary tectonics of the Fucino basin and surrounding areas (central Italy). G. Geol. 56, 73–99.
Galadini, F., Galli, P., Giraudi, C., Molin, D., 1995. Il terremoto del 1915 e la sismicità della Piana del Fucino (Italia centrale). Boll. Soc. Geol. Ital. 114, 635–663.
Galadini, F., Galli, P., Giraudi, C., 1996. Geological investigations of Italian earthquakes: new paleoseismological data from the Fucino Plain (central Italy). J. Geodyn. 24, 87–103.
Galadini, F., Galli, P., Giraudi, C., 1997. Paleosismologia della Piana del Fucino (Italia centrale). Il Quaternario 10, 27–64.
Galadini, F., Giraudi, C., Messina, P., 1999. Nuovi dati sulla tettonica tardopleistocenica dell'alta valle del Sangro (Appennino centrale): implicazioni sismotettoniche. Il Quaternario 12, in press.
Galli, P., Ferreli, L., 1995. Methodological approach for historical liquefaction researches. In: Serva, L., Slemmons, D.B. (Eds.), Perspectives in Paleoseismology. Association of Engineering Geologists, Spec. Publ. 6, Sudbury, MA, pp. 35–48.
Gasparini, C., Iannaccone, G., Scarpa, R., 1985. Fault-plane solutions and seismicity of the Italian Peninsula. Tectonophysics 117, 59–78.
Giraudi, C., 1986. Faglie ad attività olocenica nella Piana del Fucino. Mem. Soc. Geol. Ital. 35, 875–880.
Giraudi, C., 1988. Evoluzione geologica della Piana del Fucino (Abruzzo) negli ultimi 30.000 anni. Il Quaternario 1, 131–159.
Giraudi, C., 1995. Considerations on the significance of some post-glacial fault scarps in the Abruzzo Apennines (central Italy). Quat. Int. 25, 33–45.
Giraudi, C., 1998. Evoluzione geologica tardo-pleistocenica ed olocenica della Piana del Fucino e dei versanti adiacenti: analisi di nuovi dati stratigrafici e radiometrici e ricostruzione delle variazioni ambientali. In: Castenetto, S., Galadini, F. (Eds.), Il terremoto del 13 gennaio 1915. Servizio Sismico Nazionale, Rome (in press).
Giraudi, C., Frezzotti, M., 1995. Paleoseismicity in the Gran Sasso massif (Abruzzo, central Italy). Quat. Int. 25, 81–93.
Giraudi, C., Frezzotti, M., 1998. Segnalazione di stalattiti fratturate nella grotta-riparo Continenza di Trasacco: nuovi indizi di paleosismicità. In: Castenetto, S., Galadini, F. (Eds.), Il terremoto del 13 gennaio 1915. Servizio Sismico Nazionale, Rome (in press).
Kieffer, G., 1979. L'activité de l'Etna pendant le derniers 20.000 ans. C. R. Acad. Sci. Paris 288 D, 1023–1026.
Kostrov, V.V., 1974. Seismic moment and energy of earthquakes and seismic flow of rock. Izv. Akad. Sci. USSR Phys. Solid Earth, engl. transl. 10, 23–40.
Loperfido, A., 1919. Indagini astronomico-geodetiche relative al fenomeno sismico nella Marsica. Pubblication of Ministero LL. PP., Firenze, 94 pp.
Margottini, C., Ambraseys, N.N., Screpanti, A., 1993. La mag-

nitudo dei terremoti italiani del XX secolo. ENEA, Rome, 57 pp.

Messina, P., 1996. Tettonica mesopleistocenica dei terrazzi nord-orientali del Fucino (Italia centrale). Il Quaternario 9, 293–298.

Micci, A., Zaghini, M., Zecchi, R., 1975. Osservazioni sui terremoti della regione italiana e su alcuni meccanismi focali. Boll. Soc. Geol. Ital. 94, 1595–1602.

Michetti, A.M., Brunamonte, F., Serva, L., Vittori, E., 1996. Trench investigations of the 1915 Fucino earthquake fault scarps (Abruzzo, Central Italy): geological evidence of large historical events. J. Geophys. Res. 101, 5921–5936.

Mostardini, F., Merlini, S., 1986. Appennino centro meridonale, sezioni geologiche e proposta di modello strutturale. 73th Congress of the Italian Geological Society, AGIP Press, Rome, 59 pp.

Narcisi, B., 1993. Segnalazione di un livello piroclastico di provenienza etnea nell'area del Fucino (Italia centrale). Il Quaternario 6, 87–92.

Oddone, E., 1915. Gli elementi fisici del grande terremoto marsicano-fucense del 13 gennaio 1915. Boll. Soc. Sismol. Ital. 19, 71–216.

Pantosti, D., Schwartz, D.P., Valensise, G., 1993. Paleoseismology along the 1980 surface rupture of the Irpinia fault: implications for earthquake recurrence in the Southern Apennines, Italy. J. Geophys. Res. 98, 6561–6577.

Pantosti, D., D'Addezio, G., Cinti, F.R., 1996. Paleoseismicity of the Ovindoli-Pezza fault, central Apennines, Italy: a history including a large, previously unrecorded earthquake in the Middle Ages (860–1300 A.D.) J. Geophys. Res. 101, 5937–5959.

Radmilli, A.M., 1981. Storia dell'Abruzzo dalle origini all'Età del Bronzo. Giardini, Pisa, 451 pp.

Serva, L., Blumetti, A.M., Michetti, A.M., 1986. Gli effetti sul terreno del terremoto del Fucino (13 Gennaio 1915); tentativo di interpretazione della evoluzione tettonica recente di alcune strutture. Mem. Soc. Geol. Ital. 35, 893–907.

Stuiver, M., Reimer, P.J., 1993. Extended ^{14}C data base and revised CALIB 3.0 ^{14}C calibration program. Radiocarbon 35, 215–230.

Vittori, E., Cavinato, G.P., Miccadei, E., 1995. Active faulting along the northeastern edge of the Sulmona basin, central Apennines, Italy. In: Serva, L., Slemmons, D.B. (Eds.), Perspectives in Paleoseismology. Association of Engineering Geologists, Spec. Publ. 6, Sudbury, MA, pp. 115–126.

Ward, S.N., Valensise, G., 1989. Fault parameters and slip distribution of the 1915 Avezzano, Italy, earthquake derived from geodetic observations. Bull. Seismol. Soc. Am. 79, 690–710.

Wells, D.L., Coppersmith, K.J., 1994. New empirical relationships among magnitude, rupture length, rupture width, rupture area, and surface displacement. Bull. Seismol. Soc. Am. 84, 974–1002.

Westaway, R., 1992. Seismic moment summation for historical earthquakes in Italy: tectonic implications. J. Geophys. Res. 97, 15437–15464.

Zimmermann, D.W., 1971. TL dating using fine grains from pottery. Archaeometry 13, 29–59.